infection. Previous studies have shown that the presence of MAC has a clinical relevance of around 35-42% [5,6]. According to guidelines of the American Thoracic Society (ATS) [1], the diagnosis of pulmonary disease due to Mycobacterium avium complex (MAC) is based on clinical, radiographic, and mycobacterial criteria. Thus, the entire process is complicated and time consuming, requiring clinical findings and repeated MAC isolation/culture from sputum.

Moreover, it is very difficult to discriminate between MAC contamination and MAC-LD [7,8], or between MAC-LD and other mycobacterial infections without culture results. Clinical features such as symptomatic or radiographic findings are very similar in mycobacterial diseases. From the standpoint of infection control, it is particularly important to distinguish between MAC-LD and pulmonary tuberculosis (TB). Therefore, tests that can rapidly and accurately differentiate between MAC-LD and MAC contamination are needed.

Among sero-diagnostic methods, detection of serum immunoglobulin A (IgA) antibody against MAC glycopeptidolipid (GPL), an important antigenic component of MAC bacterial wall, has been recently developed. It shows good diagnostic performance in Japan (MAC-GPL IgA, Tauns Laboratory Inc., Shizuoka, Japan) [9,10]. However, a study conducted in the United States reveals that the test is specific but less sensitive (70%) when the same cut-off value (0.7 U/mL) is used, despite sufficient sensitivity (80%) obtained at 0.3 U/mL as the cut-off value [11]. The studies in Japan have included immunocompetent patients, but a small number of immunocompromised patients such as lung cancer, and did not examined patients with diseases due to rapidly growing mycobacteria (RGM) possessing glycopeptidolipid antigen such as *M. abscessus*, *M. fortuitum*, and *M. chelonae* [9,10]. Therefore, the sero-diagnostic test requires validation in different ethnicities and geographic locations with variable background prevalence of *M. tuberculosis* and NTM. This study examined the clinical availability of the sero-diagnostic test for MAC-GPL IgA, including sensitivity and specificity, in Taiwan.

Materials and Methods

Patient enrollment

This prospective study was conducted at National Taiwan University Hospital in Taipei from January 2011 to January 2013. The hospital's research ethics committee approved the study and all participants provided written informed consent. Patients aged >20 years and had respiratory sample(s) culture-positive for NTM were identified. Among them, we enrolled patients with MAC-LD, MAC contamination, rapidly growing mycobacteria (RGM, including *M. abscessus*, *M. fortuitum*, and *M. chelonae*)-LD or *M. kansasii*-LD diagnosed according to the ATS diagnostic guideline [1]. Patients with culture-proven pulmonary TB and their household contacts who had a result of interferon-gamma release assay (IGRA) but no clinical symptoms and radiographic findings suggestive for active pulmonary disease in the last 6 months were also enrolled. In this study, IGRA was performed by using T-SPOT.*TB* (Oxford Immunotech Ltd, Oxford, UK) [12]

Mycobacterial culture and species identification was performed as previously described [13]. Patients with human immunodeficiency virus (HIV) infection and bleeding tendency that increased the risk of blood sampling were excluded.

MAC-GPL IgA antibody measurement

All samples were stored in -20°C and examined in random order by a technician blinded to the patients' clinical diagnoses. Serum MAC-GPL IgA was measured by an enzyme immunoassay kit (Tauns Laboratory Inc., Shizuoka, Japan) according to the manufacturer's instructions. Data was expressed as U/mL in reference to standard curve using positive controls.

Data collection

Clinical data, including age, sex, co-morbidities, history of pulmonary TB, and laboratory data at enrollment was recorded in a standardized case report form. Disease duration was defined as the period between the date of the first confirmed positive culture and the date of patient enrollment with NTM-LD and pulmonary TB. Typical histology of NTM infection included granulomatous inflammation and/or presence of acid fast bacilli [1]. Chest imaging was interpreted as noted in a previous study [3]. Radiographic patterns of the main pulmonary lesion were categorized as consolidative, fibro-cavitary, or nodular-bronchiectatic.

Statistical analysis

Inter-group differences were analyzed by the student *t* test or Mann-Whitney *U* test for numerical variables, and chi-square test or Fisher's exact test for categorical variables, as appropriate. Multivariate logistic regression analysis was applied to identify factors associated with MAC-LD. In the stepwise variable selection procedure, all potential predictors were included. Statistical significance was set at a two-sided $p<0.05$.

The discriminative power of each significant predictor between MAC-LD and other groups or MAC contamination was compared using the receiver operating characteristic (ROC) curve and the area under the curve (AUC). The optimal cut-off value, defined as the one with the least $(1 - \text{sensitivity})^2 + (1 - \text{specificity})$, was used to calculate sensitivity and specificity [14]. All analyses were performed using the SPSS (Version 15.0, Chicago, IL).

Results

The study enrolled 56 patients with MAC-LD, 11 with MAC contamination, 14 with *M. kansasii*-LD, 26 with RGM-LD (14 *M. abscessus*, 7 *M. fortuitum*, and 5 *M. chelonae*), 48 with pulmonary TB, and 42 TB household contacts. Among the 42 household contacts, 22 (19 without underlying disease) were IGRA-positive and the remaining 20 (18 without underlying disease) were IGRA-negative.

Among the MAC-LD patients, the mean age was 67.8 years, 50% were male, and 32% had co-morbidity (Table 1). Seven MAC-LD patients had malignancies, including two with lung cancer and one each with buccal cancer, leukemia, hepatoma,

cholangiocarcinoma, and bladder cancer. Among the 56 MAC-LD patients, respiratory specimens were smear-positive for acid-fast bacilli in 33 (59%), including 10 with high-grade (3+~4+) positivity. Fifty one MAC-LD patients had ≥2 sputum samples culture-positive for MAC (average, 5.2 sets [SD: 2.8]). In five MAC-LD patients with only one positive sputum culture, four had typical lung histology and the remaining one had one bronchial washing culture positive for MAC. Based on the radiographic pattern, six (11%), nine (16%), and 41 (73%) were classified as consolidative, fibro-cavitary, and nodular-bronchiectatic lung diseases, respectively.

Among patients with MAC contamination, the mean age was 60.9 years and 64% were male. All had ≥3 sets of sputum for acid-fast smear and mycobacterial culture. Except for one who had three culture-positive sputum samples but normal chest radiography, all of the patients had only one culture-positive sputum sample. Two of the 11 persons with MAC contamination had low-grade positive acid-fast smear.

Patients with MAC-LD were older than those with *M. kansasii*-LD, pulmonary TB, and TB contacts (Table 1). Disease duration was 13.2 months in average in the MAC-LD group and this was longer than those in the *M. Kansasii*-LD, RGM-LD, and pulmonary TB groups. In the MAC-LD group, 24 patients (42%) had disease duration less than 3 months, including 10 who were started on anti-MAC treatment upon enrollment. Prior TB history was more common in the NTM-LD group than in the PTB and control groups. Laboratory data, including blood hemoglobin and leukocyte count, were similar among all groups.

Regarding MAC-GPL IgA, MAC-LD patients had significantly higher serum levels than all of the other groups (Figure 1). Multivariate logistic regression revealed that age (odds ratio [OR]: 1.032; 95% CI: 1.005-1.060), presence of autoimmune disease (OR: 4.884; 95% CI: 1.038-22.971), and serum MAC-GPL IgA antibody level (OR: 1.325; 95% CI: 1.144-1.536) were independent predictors of MAC-LD (Table 2). As regards patients with respiratory specimen(s) culture-positive for MAC, only MAC-GPL IgA level (OR: 2.856; 95% CI: 1.045-7.805) remained a significant factor for differentiating MAC-LD from MAC contamination.

The ROC curve analysis revealed that serum MAC-GPL IgA had high discriminative power for MAC-LD from all other groups (AUC 0.805, $p<0.001$) (Figure 2A), all other groups except RGM-LD (AUC 0.821, $p<0.001$) (Figure 2B), or MAC contamination (AUC 0.782; $p=0.003$) (Figure 2C). For discriminating MAC-LD from all other groups, the optimal cut-off value of serum MAC-GPL IgA was 0.26 U/ml (sensitivity 79%; specificity 76%). If the cut-off value was increased to 0.7 U/mL by the manufacturer's instruction, sensitivity and specificity became 61% and 87%, respectively.

For discriminating MAC-LD from all other groups except RGM-LD, the optimal cut-off value of MAC-GPL IgA was 0.26 U/ml (sensitivity 79%; specificity 80%). The optimal cut-off value of MAC-GPL IgA to discriminate MAC-LD from MAC contamination was 0.73 U/mL (sensitivity 60%; specificity 91%). If the cut-off value was lowered from 0.73 to 0.30 U/mL, sensitivity increased to 75% but specificity decreased to 64%.

Table 1. The participants' clinical characteristics based on lung disease status.

	MAC-LD n=56	MAC contamination n=11	*M. kansasii*-LD n=14	RGM-LD** n=26	PTB n=48	TB contacts n=42
Age (years)	67.8 [16.0]	60.9 [18.5]	56.9 [17.4]*	67.0 [13.3]	60.9 [17.9]*	50.1 [18.5]*
Male gender	28 (50%)	7 (64%)	11 (79%)	16 (62%)	32 (67%)	13 (31%)
Disease duration (months)	13.2 [21.8]	-	2.9 [8.2]*	4.3 [7.5]*	1.3 [1.1]*	-
Underlying co-morbidity	18 (32%)	4 (36%)	3 (21%)	9 (35%)	23 (48%)	5 (12%)*
Diabetes mellitus	4 (7%)	1 (9%)	1 (7%)	3 (12%)	7 (15%)	3 (7%)
Malignancy***	7 (13%)	1 (9%)	1 (7%)	2 (8%)	9 (19%)	2 (5%)
Hemodialysis	0	1 (9%)*	0	2 (8%)*	3 (6%)	0
Autoimmune diseases****	5 (9%)	0	1 (7%)	0	2 (4%)	0*
Liver cirrhosis	2 (4%)	1 (9%)	0	2 (8%)	8 (17%)*	0
Past TB history	8 (14%)	2 (18%)	4 (29%)	1 (4%)	0*	0*
MAC GPL antibody, U/mL	4.27 [6.32]	0.45 [0.73]*	0.16 [0.15]*	1.11 [2.27]*	0.78 [2.47]*	0.28 [0.74]*
Leukocytes, per μL	6926 [2743]	7045 [2225]	9063 [5082]	7528 [3628]	7661 [3658]	-
Hemoglobin, g/dL	12.6 [2.1]	12.6 [2.5]	12.2 [2.3]	12.2 [2.2]	12.7 [2.0]	-

Abbreviations: GPL, glycopeptidolipid; LD, lung disease; MAC, *Mycobacterium avium* complex; NTM, non-tuberculous mycobacteria; PTB, pulmonary tuberculosis; RGM, rapidly-growing mycobacteria

Data are no. (%) or mean [standard deviation]

*. $p<0.05$ between the indicated group and the MAC-LD group

**. RGM includes 14 *M. abscessus*, 7 *M. fortuitum*, and 5 *M. chelonae*

***. Malignancy includes 5 lung cancer, 4 head and neck cancer, 3 leukemia, 3 hepatoma, 2 breast cancer, 2 bladder cancer, 2 biliary tract cancer, and 1 thyroid cancer

Autoimmune diseases includes 3 rheumatoid arthritis, and each one of systemic lupus erythematosus, ankylosing spondilytis, Sjögren syndrome, Graves' disease, and autoimmune related nephrotic syndrome

doi: 10.1371/journal.pone.0080473.t001

Using the cut-off value of 0.73 U/ml for discriminating MAC-LD from all other groups, sensitivity was 61% and specificity 88%.

The proportion of sero-positive cases using 0.73 U/ml as the cut-off value in each group was shown in Table 3. Seven (27%) RGM-LD patients had positive MAC-GPL IgA test. The false-positive rate in RGM-LD patients was significantly higher than that in *M. kansasii*-LD patients ($p=0.025$) and TB household contacts ($p=0.033$), and borderline higher than that in pulmonary TB ($p=0.066$) patients. None of the IGRA-positive TB household contacts had a positive result of the MAC-GPL

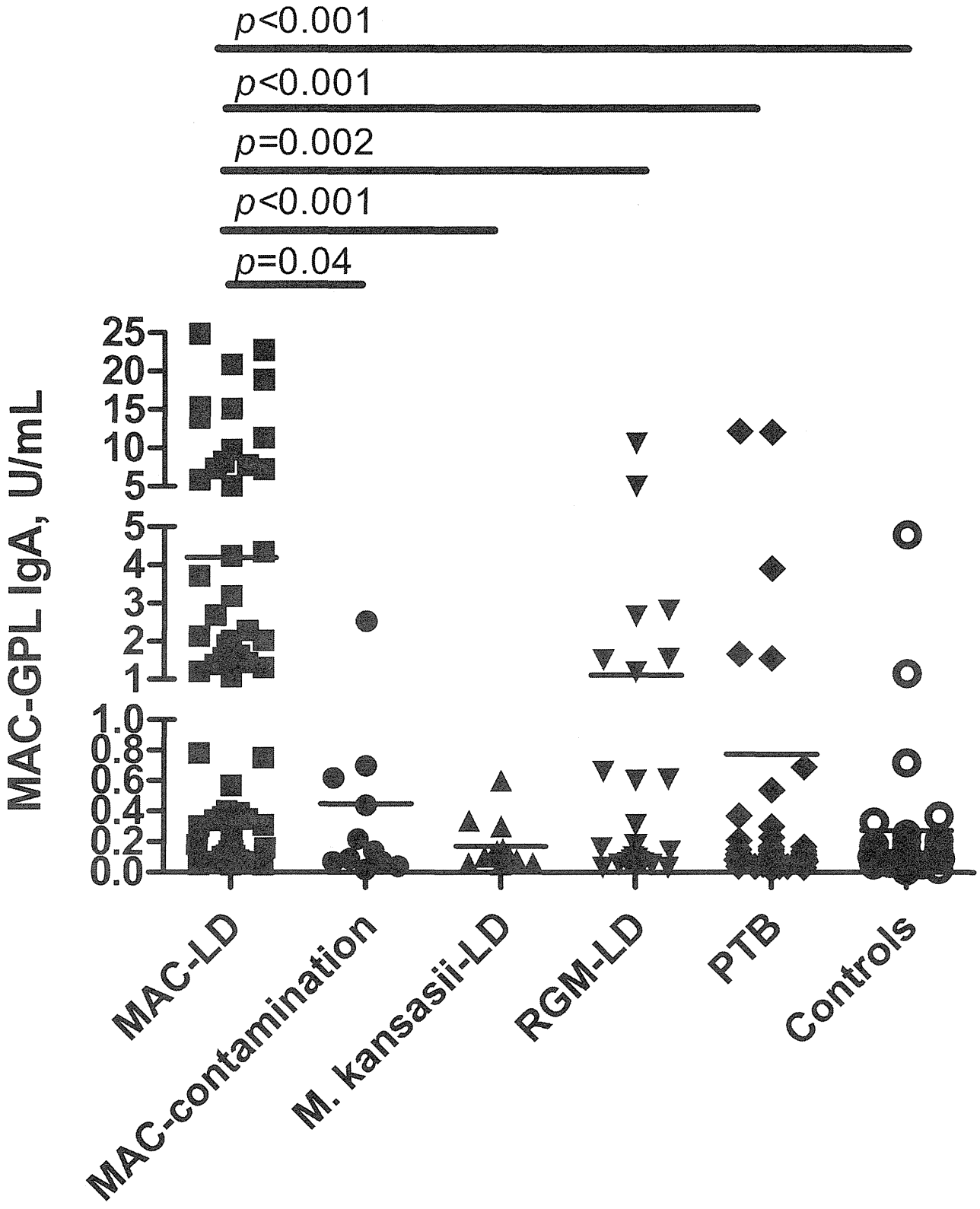

Figure 1. Serum immunoglobulin A antibody levels of Mycobacterium avium complex (MAC) glycopeptidolipid (GPL) in different lung disease statuses. IgA, immunoglobulin A; LD, lung disease; PTB, pulmonary tuberculosis; RGM, rapid-growing mycobacteria.

doi: 10.1371/journal.pone.0080473.g001

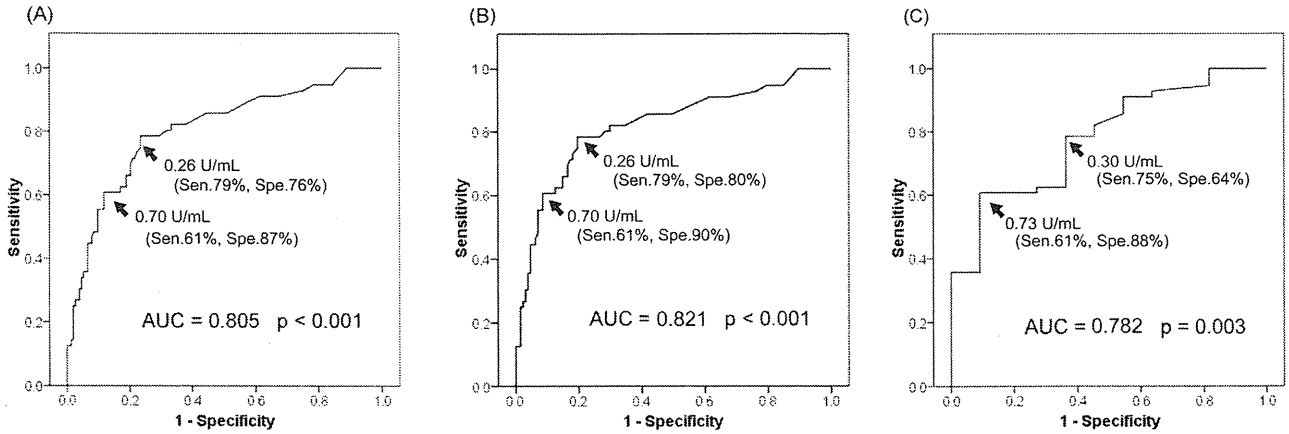

Figure 2. The receiver operating characteristic (ROC) curves were plotted for predicting patients with Mycobacterium avium complex (MAC)-lung disease in different population. (**A**) all participants, (**B**) all except RGM-LD patients, and (**C**) those with positive sputum culture for MAC. The numbers in parenthesis represent the corresponding sensitivity and specificity using the specific cut-off value. AUC, area under curve; Sen, sensitivity; Spe, specificity.

doi: 10.1371/journal.pone.0080473.g002

Table 2. Factors associated with Mycobacterium avium complex-lung disease (MAC-LD), by multivariate logistic regression.

Characteristics	Multivariate	
	p value	OR (95% C.I.)
Age, per year increment	0.020	1.032 (1.005 ~ 1.060)
Sex, male	0.204	
Presence of underlying co-morbidity	0.341	
Malignancy	0.921	
Diabetes mellitus	0.270	
Liver cirrhosis	0.339	
Hemodialysis (chronic renal failure)	0.999	
Autoimmune disease	0.045	4.884 (1.038 ~ 22.971)
Blood leukocyte count, per L	0.236	
Hemoglobin, per g/dL	0.335	
MAC GPL antibody, per U/mL increment	<0.001	1.325 (1.144 ~ 1.536)

Abbreviation: GPL, glycopeptidolipid

doi: 10.1371/journal.pone.0080473.t002

Table 3. Number and proportion of sero-positive subjects in each group based on the cut-off value of 0.73 U/ml for *Mycobacterium avium* complex glycopeptidolipid antibody.

Clinical diagnosis	Sero-positive, n (%)
MAC-LD (n=57)	34 (60%)
MAC contamination (n=11)	1 (9%)
M. kansasii-LD (n=13)	0
RGM-LD (n=26)	7 (27%)
Pulmonary TB (n=48)	5 (10%)
TB household contacts (n=42)	2 (5%)

Abbreviations: LD, lung disease; MAC, *Mycobacterium avium* complex; RGM, rapid-growing mycobacteria; TB, tuberculosis

doi: 10.1371/journal.pone.0080473.t003

IgA, whereas two (11%) of the 18 IGRA-negative contacts without underlying disease did.

In MAC-LD, patients with co-morbidity had lower MAC-GPL antibody levels than those without (1.50 vs. 5.54 IU/ml, p=0.009) and patients with malignancy had lower serum GPL IgA levels than those without (0.40 vs. 4.70 IU/ml, p=0.018). Within the MAC-LD group, patients with high smear grade had higher serum MAC-GPL IgA levels than those with low smear grade and negative smear (7.89 vs. 3.41 IU/mL, p=0.039). The MAC-GPL IgA serum level was borderline higher in 46 MAC-LD patients with ≥2 positive sputum cultures for MAC within six months before blood sampling, compared to the other 10 MAC-LD patients (4.76 vs. 2.01 U/mL, p=0.072). The ROC curve predicting those with ≥2 sputum cultures positive for MAC within six months from all participants with any sputum positive for MAC revealed that serum MAC-GPL IgA had good discriminative power (AUC 0.728, p=0.005) with the optimal cut-off value of 0.73 U/mL (sensitivity 63%; specificity 78%).

The median MAC-GPL IgA serum level was similar between those with and without prior TB history (1.32 vs. 1.47 U/ml, p = 0.982 by Mann-Whitney U test). The number of positive culture, disease duration before blood sampling, started NTM treatment, and radiographic pattern were not significantly correlated with MAC-GPL IgA level. Among the 56 MAC-LD patients, the average MAC-GPL IgA was similar in the 10 with bronchoscopic specimen(s) positive for MAC and the other 46 without (4.11 vs. 4.99 U/mL, p=0.694).

In multivariate analysis for MAC-GPL IgA ≥0.73 U/ml in MAC-LD, the presence of co-morbidity was the only independent factor (OR: 0.218; 95% CI: 0.063-0.754) (p=0.016) whereas positive culture for MAC ≥3 sets was a borderline predictor (OR: 3.530; 95% CI: 0.866-14.395) (p=0.079).

Discussion

In the present study, serum MAC-GPL IgA level is higher in MAC-LD than MAC contamination and other mycobacterial lung diseases. Using a cut-off value of 0.73 U/ml leads to an intermediate sensitivity but excellent specificity for identifying patients with MAC-LD. In MAC-LD, immuno-competence is independently associated with higher serum MAC-GPL IgA level.

Inflammatory markers like C-reactive protein, procalcitonin, and interferon-gamma are poorly associated with NTM-LD. Soluble triggering receptors expressed on myeloid cell-1 have better correlation with NTM-LD though these are not pathognomonic [7]. In contrast, MAC-GPL antibody is more specific to MAC-LD and has been developed since the last decade [9,10]. Such GPL belong to a class of glycolipids produced by several NTM [15,16] and is an important element in NTM cell wall. GPL is located in the outmost layer, and is thus very antigenic [16]. A previous study conducted in a Japanese population reported 100% specificity and 84% sensitivity in differentiating MAC-LD from other lung disease using a cut-off value of 0.7 U/ml for MAC-GPL IgA serum level [10]. Such finding suggests that GPL of MAC is antigenic and its antibody maybe a good diagnostic marker.

However, in a study conducted in the United States, the sensitivity of MAC-GPL IgA for diagnosing MAC-LD from contamination is only 51.7% and 70.1% using cut-off values of 0.7 and 0.3 U/ml, respectively [11]. Similarly, the present study shows that MAC-GPL IgA has an intermediate sensitivity but an excellent specificity for discriminating MAC-LD using a cut-off value of 0.73 U/ml. It is not sensitive enough to be diagnostic for MAC-LD in clinically suspected cases because of the high false-negative rate.

The sub-optimal sensitivity of the MAC-GPL IgA test may be explained by two reasons. First, previous studies mainly included immunocompetent patients but 32% of the MAC-LD patients in this study had some degree of immuno-compromise, which was associated with lower GPL antibody. The finding is similar to the study conducted in the US wherein 21% of the enrolled subjects were given immuno-suppressants. In the MAC-LD patients here, immuno-compromised disease such as malignancy was a major factor associated with low MAC-GPL IgA serum level. The average MAC-GPL IgA in the present study was around 4.3 U/ml, far less than the 10.7 U/ml reported in the study in Japan. Because immuno-compromised hosts have a higher probability of MAC-LD, further large-scale prospective studies are required to evaluate diagnostic performance in a population with different co-morbidity. Second, the interval of sputum positivity may matter. The MAC-LD patients without ≥2 positive sputum culture within the last six months had lower MAC-GPL IgA level, suggesting that proper timing after sputum positivity might be needed to apply this sero-diagnostic test.

The discriminative power of MAC-GPL IgA test between MAC-LD and RGM-LD is poor. The seropositivity rate is around 27% in diseases due to RGM, probably because GPL is also a cell wall component in RGM [17]. Since culture turn-around-time for RGM is usually less than one week [1], the diagnosis of RGM-LD can possibly be immediately excluded in suspected cases of MAC-LD. The specificity of MAC-GPL IgA test, therefore, increases if patients with RGM-LD are excluded. For the other groups, the false-positive rate is ≤10%, which is comparable to those of previous reports [9,11]. This may be explained by the immune response due to prior or asymptomatic MAC infection [18]. Given the possible existence of false-positive results, MAC-GPL IgA is not a suitable diagnostic test for MAC-LD before the initial mycobacterial data becomes available.

For a case of MAC contamination that is sero-positive for MAC-GPL IgA antibody, MAC-LD may be underestimated because of the low sensitivity of the ATS diagnostic criteria, especially when the patient is unable to produce/expectorate adequate sputum. However, anti-MAC chemotherapy is not recommended until the diagnosis of MAC-LD has been confirmed due to the possibility of adverse events [1,19]. The serologic test for MAC-GPL IgA may thus be useful for patients who have a respiratory sample culture-positive for MAC but in whom invasive diagnostic procedures may be risky.

The present study has some limitations. First, the case number studied is small, precluding a firm conclusion on the clinical usefulness of the MAC-GPL IgA test. The diagnostic strategy for each sub-group with different underlying diseases should also be proven by a large-scale study in the future. Second, since persons with MAC contamination are usually asymptomatic, enrolling them into the study is much more difficult than enrolling MAC-LD patients. Therefore, the number of cases of MAC contamination is particularly small. Third, although TB household contacts were free of active lung disease, they may have been exposed to MAC. Lastly, because the study was conducted in a tertiary referral center, the prevalence of co-morbidity was high, thus limiting the external generalization of the study.

In conclusion, serum level of MAC-GPL IgA antibody is higher in MAC-LD than MAC contamination and other lung diseases. Using a cut-off value of 0.73 U/mL leads to an intermediate sensitivity (60%) but good specificity (91%) for differentiating MAC-LD from MAC contamination. This might be helpful in suggesting pulmonary infection by MAC when a respiratory specimen was culture-positive for MAC but further invasive diagnostic procedure like bronchoscopy is risky. Careful consideration is needed while using MAC-GPL IgA antibody in immuno-compromised hosts.

Acknowledgements

The authors thank the staff of the Eighth Core Lab of the Department of Medical Research of National Taiwan University Hospital for their technical support.

Author Contributions

Conceived and designed the experiments: JYW KK. Performed the experiments: CCS JTW RJ MA HCL. Analyzed the data: CCS JTW MA. Contributed reagents/materials/analysis tools: CCS JYW KK MA. Wrote the manuscript: JYW KK CCS JTW MA HCL LNL CJY KTL.

References

1. Griffith DE, Aksamit T, Brown-Elliott BA, Catanzaro A, Daley C et al. (2007) An official ATS/IDSA statement: diagnosis, treatment, and prevention of nontuberculous mycobacterial diseases. Am J Respir Crit Care Med 175: 367-416. doi:10.1164/rccm.200604-571ST. PubMed: 17277290.
2. Lai CC, Tan CK, Chou CH, Hsu HL, Liao CH et al. (2010) Increasing incidence of nontuberculous mycobacteria, Taiwan, 2000-2008. Emerg Infect Dis 16: 294-296. doi:10.3201/eid1602.090675. PubMed: 20113563.
3. Shu CC, Lee CH, Hsu CL, Wang JT, Wang JY et al. (2011) Clinical characteristics and prognosis of nontuberculous mycobacterial lung disease with different radiographic patterns. Lung 189: 467-474. doi: 10.1007/s00408-011-9321-4. PubMed: 21956280.
4. Field SK, Cowie RL (2006) Lung disease due to the more common nontuberculous mycobacteria. Chest 129: 1653-1672. doi:10.1378/chest.129:6.1653. PubMed: 16778288.
5. Koh WJ, Kwon OJ, Jeon K, Kim TS, Lee KS et al. (2006) Clinical significance of nontuberculous mycobacteria isolated from respiratory specimens in Korea. Chest 129: 341-348. doi:10.1378/chest.129.2.341. PubMed: 16478850.
6. van Ingen J, Bendien SA, de Lange WC, Hoefsloot W, Dekhuijzen PN et al. (2009) Clinical relevance of non-tuberculous mycobacteria isolated in the Nijmegen-Arnhem region, The Netherlands. Thorax 64: 502-506. doi:10.1136/thx.2008.110957. PubMed: 19213773.
7. Shu CC, Lee LN, Wu MF, Lee CH, Wang JT et al. (2011) Use of soluble triggering receptor expressed on myeloid cells-1 in non-tuberculous mycobacterial lung disease. Int J Tuberc Lung Dis 15: 1415-1420. doi:10.5588/ijtld.10.0786. PubMed: 22283904.
8. Shu CC, Lee CH, Wang JY, Jerng JS, Yu CJ et al. (2008) Nontuberculous mycobacteria pulmonary infection in medical intensive care unit: the incidence, patient characteristics, and clinical significance. Intensive Care Med 34: 2194-2201. doi:10.1007/s00134-008-1221-6. PubMed: 18648768.
9. Kitada S, Maekura R, Toyoshima N, Fujiwara N, Yano I et al. (2002) Serodiagnosis of pulmonary disease due to Mycobacterium avium complex with an enzyme immunoassay that uses a mixture of glycopeptidolipid antigens. Clin Infect Dis 35: 1328-1335. doi: 10.1086/344277. PubMed: 12439795.
10. Kitada S, Kobayashi K, Ichiyama S, Takakura S, Sakatani M et al. (2008) Serodiagnosis of Mycobacterium avium-complex pulmonary disease using an enzyme immunoassay kit. Am J Respir Crit Care Med 177: 793-797. doi:10.1164/rccm.200705-771OC. PubMed: 18079497.
11. Kitada S, Levin A, Hiserote M, Harbeck RJ, Czaja CA et al. (2013) Serodiagnosis of Mycobacterium avium complex pulmonary disease in the United States. Eur Respir J 42: 454-460. doi: 10.1183/09031936.00098212. PubMed: 23100506.
12. Wang JY, Shu CC, Lee CH, Yu CJ, Lee LN et al. (2012) Interferon-gamma release assay and Rifampicin therapy for household contacts of tuberculosis. J Infect 64: 291-298. doi:10.1016/j.jinf.2011.11.028. PubMed: 22207002.
13. Wang JY, Hsueh PR, Jan IS, Lee LN, Liaw YS et al. (2006) Empirical treatment with a fluoroquinolone delays the treatment for tuberculosis and is associated with a poor prognosis in endemic areas. Thorax 61: 903-908. doi:10.1136/thx.2005.056887. PubMed: 16809417.
14. Lin JW, Chang YC, Li HY, Chien YF, Wu MY et al. (2009) Cross-sectional validation of diabetes risk scores for predicting diabetes, metabolic syndrome, and chronic kidney disease in Taiwanese. Diabetes Care 32: 2294-2296. doi:10.2337/dc09-0694. PubMed: 19755627.
15. Ripoll F, Deshayes C, Pasek S, Laval F, Beretti JL et al. (2007) Genomics of glycopeptidolipid biosynthesis in Mycobacterium abscessus and M. chelonae. BMC Genomics 8: 114. doi: 10.1186/1471-2164-8-114. PubMed: 17490474.
16. Schorey JS, Sweet L (2008) The mycobacterial glycopeptidolipids: structure, function, and their role in pathogenesis. Glycobiology 18: 832-841. doi:10.1093/glycob/cwn076. PubMed: 18723691.
17. Chatterjee D, Khoo KH (2001) The surface glycopeptidolipids of mycobacteria: structures and biological properties. Cell Mol Life Sci 58: 2018-2042. doi:10.1007/PL00000834. PubMed: 11814054.
18. Khan K, Wang J, Marras TK (2007) Nontuberculous mycobacterial sensitization in the United States: national trends over three decades. Am J Respir Crit Care Med 176: 306-313. doi:10.1164/rccm.200702-201OC. PubMed: 17507546.
19. Tanaka E, Kimoto T, Tsuyuguchi K, Watanabe I, Matsumoto H et al. (1999) Effect of clarithromycin regimen for Mycobacterium avium complex pulmonary disease. Am J Respir Crit Care Med 160: 866-872. doi:10.1164/ajrccm.160.3.9811086. PubMed: 10471610.

RESEARCH ARTICLE

Critical Roles for Lipomannan and Lipoarabinomannan in Cell Wall Integrity of Mycobacteria and Pathogenesis of Tuberculosis

Takeshi Fukuda,[a] Takayuki Matsumura,[b] Manabu Ato,[b] Maho Hamasaki,[c] Yukiko Nishiuchi,[d] Yoshiko Murakami,[a] Yusuke Maeda,[a] Tamotsu Yoshimori,[c] Sohkichi Matsumoto,[d] Kazuo Kobayashi,[b] Taroh Kinoshita,[a] Yasu S. Morita[a]*

Research Institute for Microbial Diseases, WPI-Immunology Frontier Research Center, Osaka University, Osaka, Japan[a]; Department of Immunology, National Institute of Infectious Diseases, Tokyo, Japan[b]; Department of Genetics, Graduate School of Medicine, Osaka University, Osaka, Japan[c]; Department of Bacteriology, Osaka City University Graduate School of Medicine, Osaka, Japan[d]

* Present address: Yasu S. Morita, Department of Microbiology, University of Massachusetts, Amherst, Massachusetts, USA.

T.F. and T.M. contributed equally to this work.

ABSTRACT **Lipomannan (LM) and lipoarabinomannan (LAM) are mycobacterial glycolipids containing a long mannose polymer. While they are implicated in immune modulations, the significance of LM and LAM as structural components of the mycobacterial cell wall remains unknown. We have previously reported that a branch-forming mannosyltransferase plays a critical role in controlling the sizes of LM and LAM and that deletion or overexpression of this enzyme results in gross changes in LM/LAM structures. Here, we show that such changes in LM/LAM structures have a significant impact on the cell wall integrity of mycobacteria. In *Mycobacterium smegmatis*, structural defects in LM and LAM resulted in loss of acid-fast staining, increased sensitivity to β-lactam antibiotics, and faster killing by THP-1 macrophages. Furthermore, equivalent *Mycobacterium tuberculosis* mutants became more sensitive to β-lactams, and one mutant showed attenuated virulence in mice. Our results revealed previously unknown structural roles for LM and LAM and further demonstrated that they are important for the pathogenesis of tuberculosis.**

IMPORTANCE **Tuberculosis (TB) is a global burden, affecting millions of people worldwide. *Mycobacterium tuberculosis* is a causative agent of TB, and understanding the biology of *M. tuberculosis* is essential for tackling this devastating disease. The cell wall of *M. tuberculosis* is highly impermeable and plays a protective role in establishing infection. Among the cell wall components, LM and LAM are major glycolipids found in all *Mycobacterium* species, show various immunomodulatory activities, and have been thought to play roles in TB pathogenesis. However, the roles of LM and LAM as integral parts of the cell wall structure have not been elucidated. Here we show that LM and LAM play critical roles in the integrity of mycobacterial cell wall and the pathogenesis of TB. These findings will now allow us to seek the possibility that the LM/LAM biosynthetic pathway is a chemotherapeutic target.**

Received 24 October 2012 **Accepted** 22 January 2013 **Published** 19 February 2013

Citation Fukuda T, Matsumura T, Ato M, Hamasaki M, Nishiuchi Y, Murakami Y, Maeda Y, Yoshimori T, Matsumoto S, Kobayashi K, Kinoshita T, Morita YS. 2013. Critical roles for lipomannan and lipoarabinomannan in cell wall integrity of mycobacteria and pathogenesis of tuberculosis. mBio 4(1):e00472-12. doi:10.1128/mBio.00472-12.

Invited Editor William Bishai, Johns Hopkins University School of Medicine

Editor Keith Klugman, Emory University

Address correspondence to Yasu S. Morita, ymorita@microbio.umass.edu.

Mycobacterium tuberculosis, an etiologic agent of tuberculosis (TB), infects around one-third of the world population and kills millions of people annually (1). A critical contributor to the ability of *M. tuberculosis* to evade the host immune system is its hydrophobic and complex cell wall, which is composed of peptidoglycan, arabinogalactan, mycolic acids, and glycolipids layered on top of the plasma membrane (2). Lipoarabinomannan (LAM), lipomannan (LM), and phosphatidylinositol (PI) mannosides (PIMs) are mannose-containing glycolipids that are important constituents of the cell envelope. These molecules have a PI membrane anchor and are embedded in the plasma membrane or the outer membrane by their lipid moiety (3). PIMs are highly heterogeneous in structure and carry up to four fatty acids and six mannoses (4, 5). The predominant forms of PIM are triacylated species termed AcPIM2 and AcPIM6, which carry two and six mannoses, respectively. LM and LAM carry a much longer chain of α-1,6-linked mannoses, and the α-1,6-mannan backbone is further modified by multiple α-1,2-monomannose branches (Fig. 1) (6). In *Mycobacterium smegmatis*, a nonpathogenic model organism, LM/LAM mannan carries 21 to 34 mannose residues (7), and in the case of LAM, the mannan backbone is further modified with arabinan(s), which consists of α-1,5-linked arabinose backbones with α-1,3 branch points.

PIMs, LM, and LAM are synthesized by sequential additions of mannoses and arabinoses to PI, one of the major phospholipids in mycobacterial plasma membranes (5, 8–10) (Fig. 1). While the initial steps of PIM/LM/LAM biosynthesis overlap, the biosynthetic pathway of LM and LAM diverges from that of AcPIM6 at

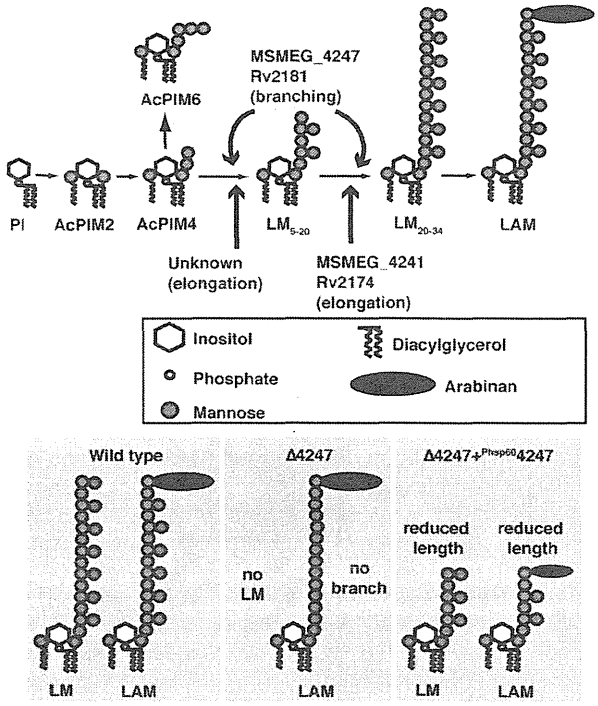

FIG 1 LM/LAM biosynthetic pathway and phenotypes of the mutants. See the text for details.

the intermediate AcPIM4 (11). PimE (MSMEG_5136) is an α-1,2-mannosyltransferase that commits AcPIM4 to the AcPIM6 pathway, and *pimE* deletion mutants cannot produce AcPIM6, while they do not have any apparent defect in LM/LAM biosynthesis (12). For the LM/LAM pathway, the elongating α-1,6-mannosyltransferase (MSMEG_4241) and branch-forming α-1,2-mannosyltransferase (MSMEG_4247) mediate mannan synthesis in *M. smegmatis* (7, 13). An *MSMEG_4241* deletion mutant accumulates an LM intermediate carrying 5 to 20 mannose residues, suggesting that there is at least one other unidentified α-1,6-mannosyltransferase involved in the initial stage of the mannan elongation. Deletion of *MSMEG_4247* resulted in ablation of branch-forming α-1,2-mannosyltransferase activities, leading to accumulation of branchless LAM and the complete absence of LM (13, 14). Interestingly, we previously reported that the overexpression of MSMEG_4247 resulted in the production of smaller LM and LAM carrying dwarfed mannan and arabinan (14). Because MSMEG_4247 is the branch-forming mannosyltransferase, we initially expected a greater frequency of monomannose side chains from overexpression strains. Production of smaller LM and LAM was therefore unexpected, and our further analysis demonstrated that the balance in the expression levels of MSMEG_4241 and MSMEG_4247 is critical for the production of properly sized LM and LAM. Our current hypothesis is that branch-forming mannosyltransferase plays a role in the termination of mannan backbone elongation, and therefore, the overproduction of MSMEG_4247 results in premature termination of the backbone elongation, leading to the production of smaller LM and LAM. In *M. tuberculosis*, Rv2174 and Rv2181 have been identified as orthologs of MSMEG_4241 and MSMEG_4247, respectively (7, 13, 15, 16). We reported that the overexpression of Rv2181 also results in phenotypes similar to those of MSMEG_4247-overexpressing *M. smegmatis* and suggested that the mannan backbone length of LM and LAM is similarly controlled in *M. tuberculosis*. A unique feature of LAM produced by pathogenic species is di- and trimannosyl capping decorating the nonreducing arabinan termini (17–19). MT1671 from *M. tuberculosis* CDC1551 (orthologous to Rv1635c in *M. tuberculosis* H37Rv) mediates the priming of the first capping mannose to the terminal arabinose (20), and subsequent α-1,2-mannosyl transfers are mediated by Rv2181 (15). Thus, while Rv2181 and MSMEG_4247 are biochemically similar enzymes, mediating the synthesis of α-1,2-monomannose side chain, Rv2181 plays an additional role in LAM mannose cap synthesis in *M. tuberculosis*. Relatively little is known about Rv2174 other than the fact that Rv2174 can complement the MSMEG_4241 deletion mutant of *M. smegmatis* (7) and that the gene is predicted to be essential (21).

While many studies have described the immunomodulatory activities of LM and LAM (22–25), their roles as structural components of the cell envelope remain elusive. A significant fraction of LM and LAM appears to be anchored to the plasma membrane (3) and therefore has its glycans positioned to interact directly with the cell wall core structure. Thus, it is reasonable to speculate that LM and LAM have a direct role in maintaining cell wall integrity. There are a few recent studies that indicated potential structural roles of LM and LAM in *M. tuberculosis*. For example, EmbC, an arabinosyltransferase involved in LAM synthesis, is an essential enzyme in *M. tuberculosis* (26), suggesting that LAM plays a fundamental role in mycobacterial physiology. Another interesting study found that levels of LM and LAM were reduced in a PimB (Rv0557)-deletion *M. tuberculosis* mutant, and this mutant became more effective in killing macrophages (27). These studies suggested that LM and LAM are important for the growth and pathogenesis of *M. tuberculosis*. We recently reported that balanced expression levels of elongating and branch-forming mannosyltransferases are important for the biosynthesis of LM and LAM with correct mannan sizes (14). In the current study, we used these mutants to examine the physiological roles of LM and LAM in the context of maintaining cell wall integrity. We found that *M. smegmatis* mutants lost their acid-fastness, became more sensitive to various antibiotics, and became more prone to macrophage killing, suggesting loss of cell wall integrity. Similarly, equivalent *M. tuberculosis* mutants became more sensitive to antibiotics, and one of them failed to establish effective infection in mice. Our data therefore indicate that LM and LAM are critical for the cell wall integrity and pathogenicity of mycobacteria.

RESULTS

Growth and viability of *MSMEG_4247* deletion and overexpression strains. We previously made *MSMEG_4247* deletion (Δ4247) and overexpression (Δ4247+^{Phsp60}4247) strains of *M. smegmatis* and reported that LM/LAM structures became aberrant (14). To investigate the impact of such changes on the cellular physiology of mycobacteria, we first examined the growth rate of these strains and found that they grew at essentially the same rate as did the parental strain (Fig. 2A). We also found no changes in viabilities of the mutants in comparison to the parental strain during 8 days of culture (Fig. 2B). These data suggested that aberrant structures of LM and LAM do not significantly affect the growth and viability of *M. smegmatis*.

Plasma membrane structure and function of *MSMEG_4247* deletion and overexpression strains. PimE, the α-1,2-

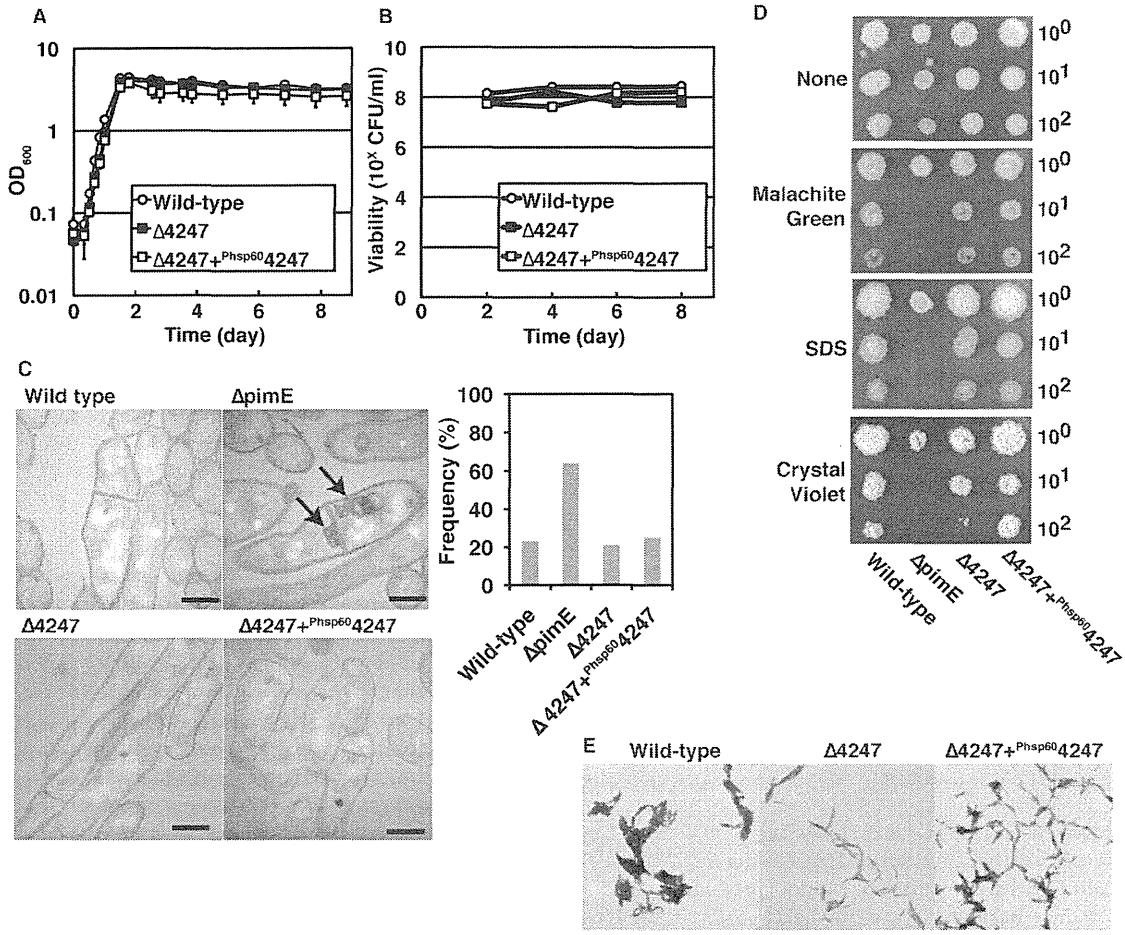

FIG 2 MSMEG_4247 deletion or overexpression results in loss of acid-fast staining. (A and B) Growth and viability of MSMEG_4247 deletion and overexpression mutants. Stationary cells were diluted 100-fold in Middlebrook 7H9 broth, and growth was monitored by OD_{600} measurement. Viability was determined by counting CFU on Middlebrook 7H10 agar plates. Experiments were performed in triplicate, and standard deviations are shown. (C) Transmission electron micrographs of Δ4247 and Δ4247+^{Phsp60}4247 strains compared to the Δ*pimE* mutant. Bars, 500 nm. The graph indicates the frequency of cells with membrane invaginations. (D) Sensitivity of *M. smegmatis* mutants to membrane-permeable compounds malachite green, SDS, and crystal violet. (E) Acid-fast staining of MSMEG_4247 deletion and overexpression mutants.

mannosyltransferase involved in AcPIM6 synthesis, is critical for the maintenance of plasma membrane structure, and a Δ*pimE* mutant developed plasma membrane invaginations (12) (Fig. 2C, arrows). In contrast, LM/LAM mutants did not show any morphological plasma membrane aberrations, and occasional membrane invaginations in the LM/LAM mutants were no more frequent than they were in wild-type cells (~20%) (Fig. 2C). These data suggested that structural changes in LM and LAM do not have significant impact on the plasma membrane morphology. We then examined the sensitivity of these mutants to chemical compounds such as malachite green, sodium dodecyl sulfate (SDS), and crystal violet. These lipophilic compounds are toxic to mycobacteria and have been used to test the permeability of the plasma membrane (28). Consistent with the morphological abnormalities of the Δ*pimE* plasma membrane, the Δ*pimE* mutant became markedly sensitive to these compounds (Fig. 2D). In contrast, LM/LAM mutants showed little change in sensitivity, suggesting that structural changes in LM and LAM do not affect the permeability of these compounds.

Acid-fastness is a hallmark of mycobacteria and has been attributed to the waxy nature of the cell wall outer membrane. We wondered if the acid-fastness is affected in our mutants. While the parental strain of *M. smegmatis* showed a typical red color following carbol-fuchsin staining, both Δ4247 and Δ4247+^{Phsp60}4247 were negative for this staining (Fig. 2E). These data suggested that the cell wall integrity of the LM/LAM mutants is compromised significantly despite the fact that these mutants are resistant to the abovementioned chemical compounds.

Catalytic activity of MSMEG_4247 is critical for changes in cell wall integrity. The expression of MSMEG_4247 driven by the Hsp60 promoter is significantly greater than the endogenous level (14). Therefore, we wished to exclude the possibility that the altered cell wall properties of Δ4247+^{Phsp60}4247 are a nonspecific effect of protein overexpression. We have previously demonstrated that the smaller LM/LAM phenotype of Δ4247+^{Phsp60}4247 can be reproduced when MSMEG_4247 is overexpressed in a wild-type background, and 15-fold overexpression is sufficient to induce this effect. We also demon-

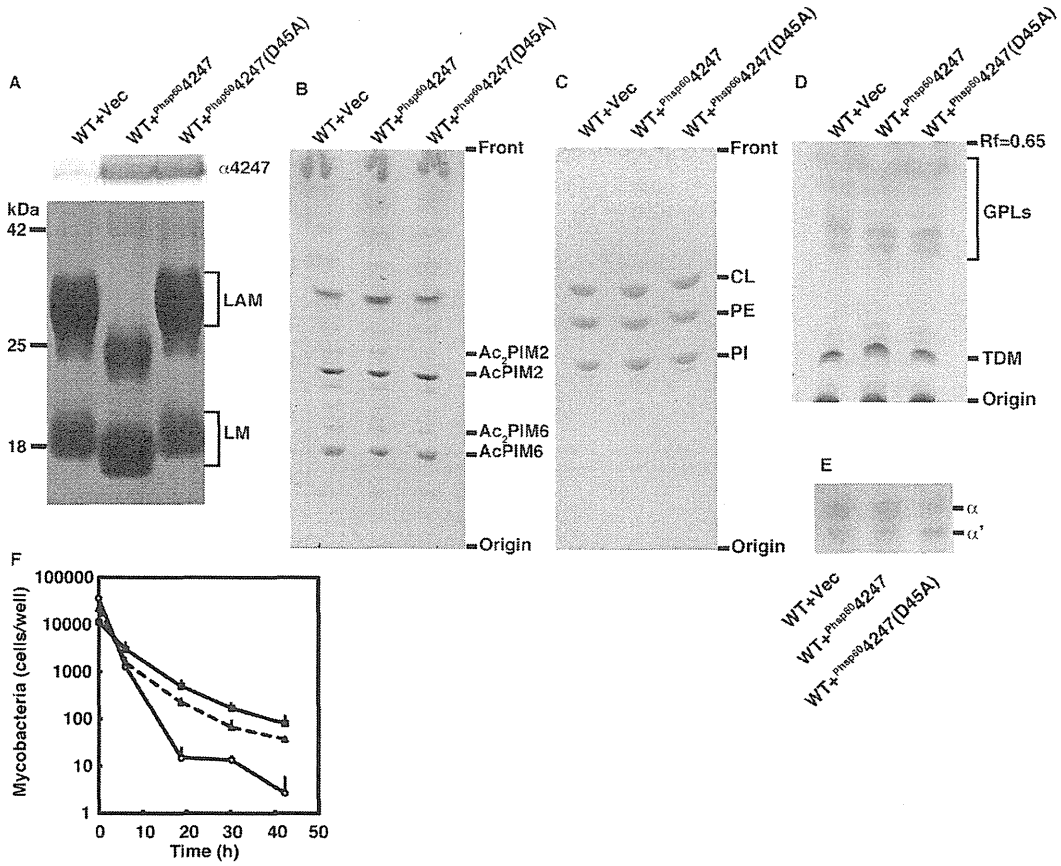

FIG 3 Catalytic activity of MSMEG_4247 is critical for the phenotype of the MSMEG_4247 overexpression mutant. (A) (Top) Western blot assay using anti-MSMEG_4247 antibody. (Bottom) ProQ Emerald staining showing LM/LAM profiles. (B) Extracted lipids were separated by high-performance thin-layer chromatography (HPTLC) using chloroform-methanol-13 M ammonia-1 M ammonium acetate-water (180:140:9:9:23) as a solvent system and stained for glycolipids using orcinol. (C) Extracted lipids were separated on an HPTLC plate using chloroform-methanol-13 M ammonia-1 M ammonium acetate-water (180:140:9:9:23) as a solvent system, and separated lipids were stained for phospholipids using molybdenum blue staining reagent. CL, cardiolipin; PE, phosphatidylethanolamine. (D) Extracted lipids were separated on an HPTLC plate using chloroform-methanol (9:1) as a solvent system, and separated lipids were visualized by orcinol staining. GPLs, glycopeptidolipids; TDM, trehalose dimycolate. (E) Mycolic acids released from the peptidoglycan-arabinogalactan core were methylated, and mycolic acid methyl ester was separated and visualized by chromic acid staining. α and α' indicate methyl ester derivatives of α-mycolic acid and α'-mycolic acid, respectively. (F) Killing of *M. smegmatis* by THP-1 cells. *M. smegmatis* WT+Vec (solid squares), WT+^{Phsp60}4247 (open circles), and WT+^{Phsp60}4247(D45A) (solid triangles with dashed line) were incubated with activated THP-1 cells, and survival of *M. smegmatis* cells was monitored by counting recovered CFU. Experiments were performed in triplicate, and standard deviations are shown.

strated that catalytically inactive MSMEG_4247 D45A mutant protein cannot induce the same effect in the same wild-type background (14). We took advantage of these observations and compared wild-type cells overexpressing catalytically active and inactive forms of the enzyme [WT+^{Phsp60}4247 and WT+^{Phsp60}4247(D45A)]. We preferred the wild-type background because deletion mutants might have additional mutations that could complicate the interpretation of our data. We first confirmed high expression levels of MSMEG_4247 by Western blotting (Fig. 3A). Consistent with our previous publication (see Fig. 2 [Δ4247 background] or Fig. 3 [wild-type background] in reference 14), LM and LAM became smaller only when the wild-type cells were transfected with catalytically active MSMEG_4247 (WT+^{Phsp60}4247) (Fig. 3A). We then examined if other components of the cell wall and plasma membrane are affected by overexpression of MSMEG_4247. We found that PIMs, phospholipids, trehalose dimycolate, and glycopeptidolipids are all present at levels comparable between the two strains (Fig. 3B to D). In addition, α and α' subspecies of mycolic acids released from the peptidoglycan-arabinogalactan-mycolic acid core were present at similar levels (Fig. 3E). These data suggested that the compositions of the cell wall and plasma membrane in these mutants were largely unchanged. We further determined the sensitivity of mutants to various antibiotics, including vancomycin and β-lactam antibiotics, using an alamarBlue growth assay. We focused on these antibiotics because these drugs primarily target peptidoglycan biosynthesis and do not have to cross the plasma membrane. We found that WT+^{Phsp60}4247 was more sensitive to vancomycin than was WT+^{Phsp60}4247(D45A) (Table 1). Furthermore, we found that WT+^{Phsp60}4247 was more sensitive to several β-lactam antibiotics such as meropenem, cefotaxime, and cefepime, although it remained resistant to other β-lactams (Table 1). Although these effects are relatively mild, these data implied that changes in LM/LAM structures substantially affected the barrier function of the cell wall. Cell

TABLE 1 Antibiotic sensitivities of *M. smegmatis* mutants[a]

Antibiotic class	Antibiotic name	IC_{50} (μg/ml)		
		Wild type + empty vector	WT+^{Phsp60}4247	WT+^{Phsp60}4247(D45A)
Glycopeptide	Vancomycin	0.27 ± 0.00	0.11 ± 0.01	0.21 ± 0.01
Penam	Ampicillin	>400	>400	>400
	Carbenicillin	>400	>400	>400
	Benzylpenicillin	>200	>200	>200
Carbapenem	Meropenem	2.6 ± 0.3	0.58 ± 0.03	1.9 ± 0.1
Cephem	Cephalothin	>200	>200	>200
	Cefamandole	>200	>200	>200
	Cefotaxime	>800	47.7 ± 8.8	>800
	Cefepime	>200	1.2 ± 0.3	>200
Monobactam	Aztreonam	>200	>200	>200

[a] Vancomycin, meropenem, cefotaxime, and cefepime values are given as means ± standard deviations from triplicate data. Other antibiotics were tested in duplicate. IC_{50}, 50% inhibitory concentration.

envelope perturbation has been suggested to be a major intracellular stress encountered by *M. tuberculosis* during infection of human THP-1 monocyte cells (29), so we considered the possibility that these LM/LAM mutants might be more sensitive to killing by THP-1 cells. Because *M. smegmatis* is nonpathogenic, the wild-type strains are susceptible to killing by activated THP-1 cells, and at least 99% of cells are killed within 42 h (Fig. 3F). When we compared our mutants, WT+^{Phsp60}4247 appeared to be phagocytosed more readily as indicated by a CFU number slightly higher than that of the wild type at time zero. Furthermore, WT+^{Phsp60}4247 was killed at a higher rate than was WT+^{Phsp60}4247(D45A) (Fig. 3F), suggesting that LM and LAM play a protective role against the bactericidal activity of THP-1 cells.

Tetracycline-inducible suppression of MSMEG_4241 expression. Continuous overexpression of MSMEG_4247 might select for an adaptive mutation that compensates for the decreased fitness due to aberrant LM/LAM structures. To minimize such a possibility of secondary mutation and examine the direct impact of LM and LAM on cell wall integrity, we created a tetracycline-inducible strain to suppress the expression of MSMEG_4241. As MSMEG_4241 mediates the elongation of mannan backbone, tetracycline-inducible suppression of its expression allowed us to examine the direct consequences of structural alterations of LM and LAM.

We designed a construct so that the reverse tetracycline repressor (revTetR)-controlled promoter controls the expression of MSMEG_4241 (Fig. 4A). Targeted integration of the construct was confirmed by Southern blotting (Fig. 4A). The revTetR expression vector was then introduced and maintained episomally. In the resultant *MSMEG_4241* Tet-off cells, MSMEG_4241 expression was reduced to undetectable levels as early as 23 h after addition of anhydrotetracycline (atc), a tetracycline analog (Fig. 4B). Both mature LM and LAM disappeared upon induction, and LM-like intermediates accumulated (Fig. 4C). Matrix-assisted laser desorption–ionization time of flight mass spectrometry (MALDI-TOF-MS) showed that these LM-like intermediates carry 9 to 18 mannoses (Fig. 4D), consistent with the intermediate species previously observed in an *MSMEG_4241* deletion mutant (7). Taken together, we have established an MSMEG_4241 Tet-off mutant that becomes unable to produce mature LM and LAM upon atc addition.

We examined the effect of MSMEG_4241 Tet-off induction on growth and found that cells grew at almost the same rate, regardless of induction (Fig. 4E). We also found no difference in the plasma membrane integrity at an ultrastructural level (Fig. 4F). Furthermore, Tet-off induction did not change the sensitivity of cells to malachite green, SDS, or crystal violet (Fig. 4G). However, consistent with the phenotypes of Δ4247 and Δ4247+^{Phsp60}4247, MSMEG_4241 Tet-off cells lost their acid-fastness upon induction (Fig. 4H). These data suggest that the structural changes of LM and LAM have a direct and immediate impact on cell wall integrity.

Changes in LM/LAM structures affect the pathogenesis of *M. tuberculosis*. We next wanted to examine if the roles that LM and LAM play in *M. smegmatis* can be extended to pathogenic species. We have previously created *M. tuberculosis* mutants that either lack or overexpress *Rv2181* (Δ2181 or Δ2181+^{Phsp60}2181, respectively) and shown that their LM/LAM profiles were aberrant in a manner similar to that of their *M. smegmatis* counterparts (Fig. 5A). Using a polyclonal antibody against Rv2181, we confirmed that Δ2181 and Δ2181+Vec lack Rv2181 expression (Fig. 5A). We also confirmed that the Δ2181+^{Phsp60}2181 strain overexpresses Rv2181 protein. The doubling time of these mutants was not significantly different from that of the wild type (Table 2). Interestingly, we also found no significant differences in acid-fastness between wild-type, Δ2181+Vec, and Δ2181+^{Phsp60}2181 strains (data not shown), possibly suggesting more dominant roles of the core mycolic acid-arabinogalactan-peptidoglycan layer for acid-fastness in *M. tuberculosis*. Nevertheless, when we tested the sensitivity of the mutants to antibiotics, we found that both Δ2181+Vec and Δ2181+^{Phsp60}2181 were more sensitive to various antibiotics (Table 3). Interestingly, *M. tuberculosis* mutants became sensitive to wider varieties of β-lactams than did *M. smegmatis* mutants (see Discussion).

This increased sensitivity to antibiotics indicated that the changes in LM/LAM structures have a significant impact on the integrity of the *M. tuberculosis* cell wall. Because the *M. smegmatis* mutant was more sensitive to macrophage killing (Fig. 3G), we

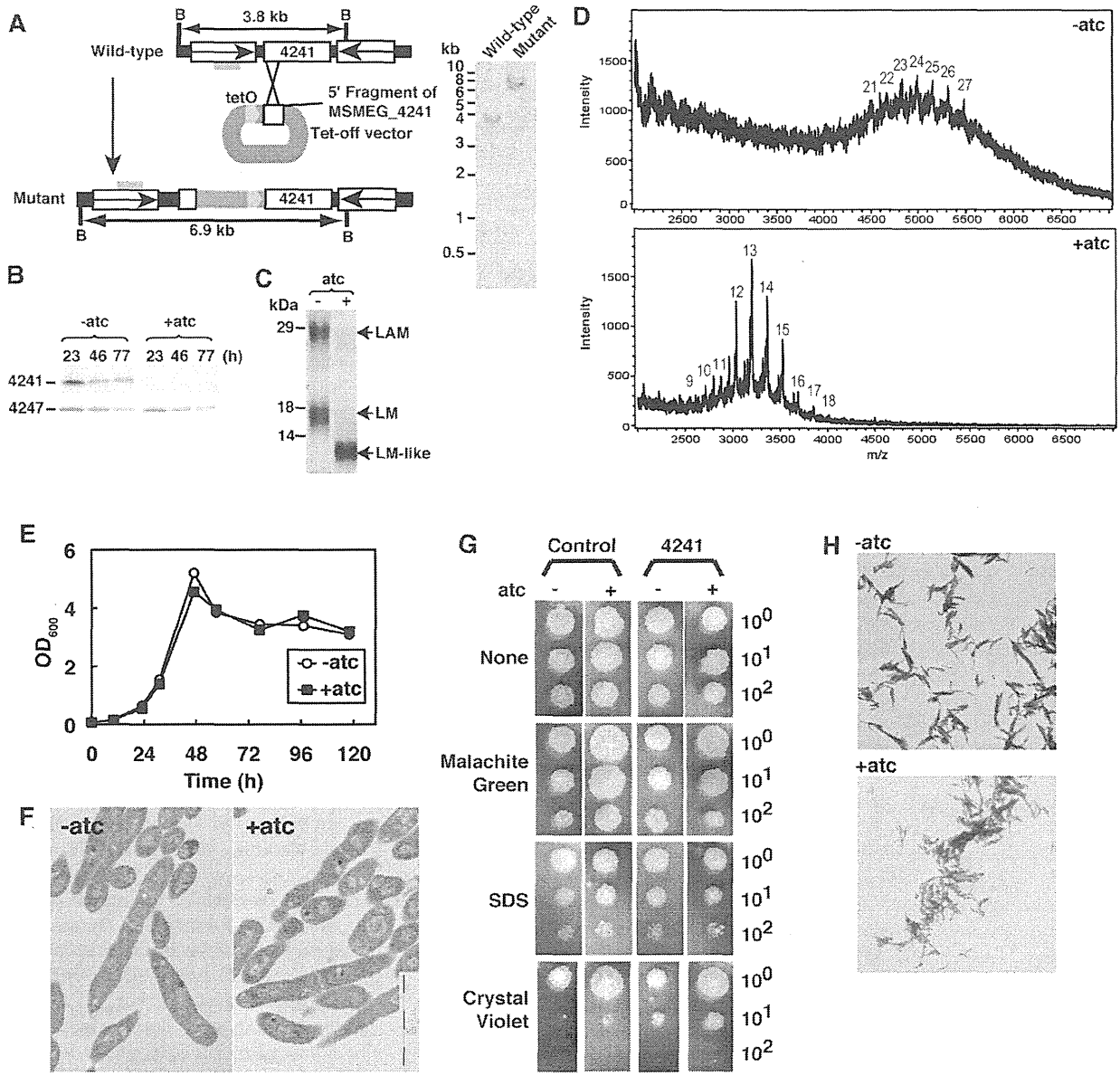

FIG 4 Establishment and analysis of MSMEG_4241 Tet-off cells. (A) Strategy to establish MSMEG_4241 Tet-off cells and Southern blot assay confirming homologous recombination. See Materials and Methods for details. B, BamHI site. The gray bar indicates the region used as a Southern blot probe. (B) Western blotting using anti-MSMEG_4241 and anti-MSMEG_4247 antibodies, showing that the expression of MSMEG_4241 was effectively turned off by the addition of atc. (C) LM/LAM profiles of Tet-off cells. LM and LAM were extracted from cells at the 23-h time point, analyzed by SDS-PAGE, and visualized by ProQ Emerald staining. (D) MALDI-TOF-MS analysis of LM accumulating at 23 h after addition of atc. The number of mannose residues is indicated for each LM peak. (E) Growth of bacteria monitored by OD_{600} in Middlebrook 7H9 broth. (F) Transmission electron micrographs of cells with or without atc induction. (G) Sensitivity of cells to malachite green, SDS, and crystal violet. For tetracycline induction, agar plates were supplemented with 40 ng/ml atc. (H) Cells at the 27-h time point were subjected to acid-fast staining.

considered the possibility that these *M. tuberculosis* mutants may show defects in infection of mice. To test this hypothesis, we intratracheally injected C57BL/6 mice with wild-type, Δ2181+Vec, and Δ2181+^{Phsp60}2181 strains and monitored bacterial growth and survival of mice. We determined the level of infection by lung CFU. We found that bacterial colonization was efficient in mice infected with either mutant strain, although we observed slightly lower lung CFU from mice infected with the Δ2181+^{Phsp60}2181 mutant, especially at 12 weeks postinfection (Fig. 5B). More strikingly, Δ2181+^{Phsp60}2181 was unable to kill the mice under the condition where mice infected with wild-type *M. tuberculosis* started to die after 6 weeks (Fig. 5C), suggesting that its virulence was significantly compromised. Because LM and LAM have been implicated in immunomodulatory activities, we monitored local inflammation and cytokine responses in the infected lungs during the course of infection. There were no clear changes in either the

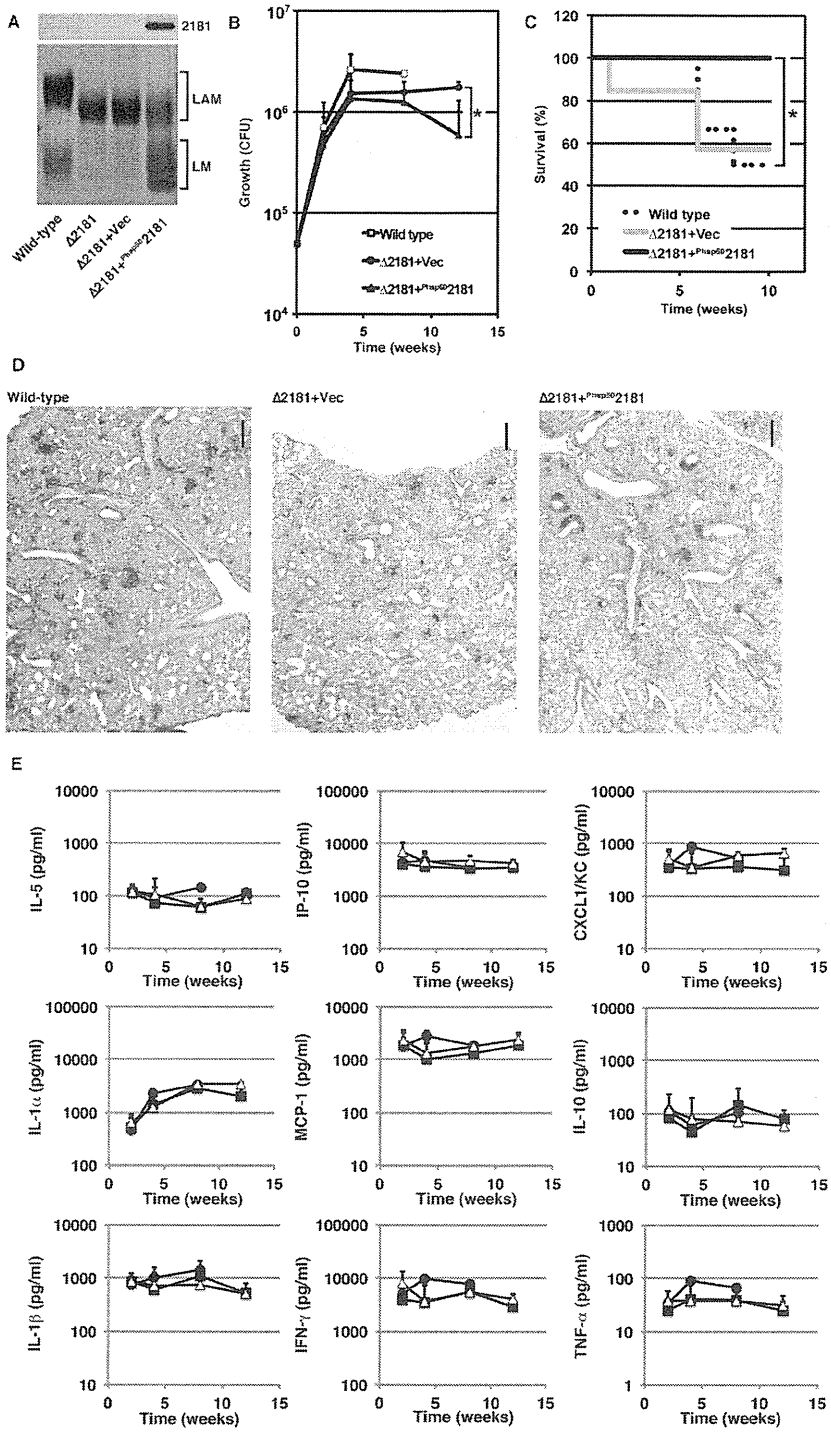

FIG 5 Phenotypes of *M. tuberculosis* mutants. (A) (Top) Western blot assay using anti-Rv2181 antibody. (Bottom) ProQ Emerald staining showing LM/LAM profiles. (B) Growth of *M. tuberculosis* mutants in mouse lung. Experiments were performed in triplicate, and the data represent the mean CFU ± standard deviation from three independent experiments on three mice for each condition. The 12-week time point for mice infected with wild-type *M. tuberculosis* was not calculated because of an insufficient number of surviving mice. Asterisk, $P < 0.05$. (C) Survival of mice after infection with *M. tuberculosis* mutants. Asterisk, $P < 0.05$. (D) Histological analysis of lung tissues infected with *M. tuberculosis* mutants for 8 weeks. In all cases, inflammatory responses such as infiltration of neutrophils and lymphocytes as well as proliferation of macrophages are evident. Bars, 1 mm. (E) Pulmonary cytokine levels during infection ($n = 3$, ±standard deviation). Solid circles, wild type; open triangles, Δ2181+Vec; solid squares, Δ2181+^{Phsp60}2181. IFN-γ, gamma interferon; TNF-α, tumor necrosis factor alpha. The data in panels B to E are representative of 2 independent experiments.

severity of inflammation (Fig. 5D) or the levels of cytokine production (Fig. 5E) between mice infected with wild-type *M. tuberculosis* and those infected with mutants. We also tested but did not detect significant production of other cytokines such as interleukin-12 p70 (IL-12p70), IL-4, IL-17, IL-2, and granulocyte-macrophage colony-stimulating factor (GM-CSF). Although we cannot eliminate the possibility that cytokines that we did not test play roles in responding to the exposure to LM and LAM, these data are consistent with the possibility that LM and LAM play a role in establishing *M. tuberculosis* infection without having dominant roles in inflammatory responses.

DISCUSSION

In this study, we examined the roles for LM and LAM in the integrity of the mycobacterial cell envelope. Structural changes in LM and LAM significantly compromised the cell wall integrity of *M. smegmatis*, as demonstrated by the loss of acid-fastness, increased sensitivity to antibiotics, and faster killing by macrophages. Similarly, defects in LM/LAM structures in *M. tuberculosis* led to increased antibiotic sensitivity and attenuated infectivity. Thus, our data demonstrate that LM and LAM are critical for maintaining cell wall integrity. In addition, while previous studies demonstrated that the deletion of *Rv2181* is not lethal in *M. tuberculosis* (14, 15), *Rv2174* is predicted to be an essential gene (21). Furthermore, *embC*, which encodes an arabinosyltransferase for LAM biosynthesis, cannot be deleted in *M. tuberculosis* (26). Taken together with these previous observations, the LM/LAM biosynthetic pathway can be considered a candidate for drug targets.

We found that changes in LM/LAM structures have a significant impact on the cell envelope integrity of both *M. smegmatis* and *M. tuberculosis*. However, there were some differences between the two species. For example, *M. smegmatis* lost the acid-fast property of the cell wall upon deletion or overexpression of MSMEG_4247, as well as tetracycline-induced downregulation of *MSMEG_4241* (Fig. 2E and 4H). In contrast, equivalent *M. tuberculosis* mutants did not show defects in the acid-fastness (not shown). These data indicate that LM and LAM do not have a significant impact

TABLE 2 Doubling time of *M. tuberculosis* mutants

M. tuberculosis strain	Doubling time (h)
Wild type	25.4 ± 1.1
Δ2181	25.0 ± 0.3
Δ2181 + empty vector	28.5 ± 1.6
Δ2181+^{Phsp60}2181	24.6 ± 0.9

on the acid-fastness of *M. tuberculosis*, which could be due to the compositional differences in the *M. tuberculosis* outer membrane. While *M. tuberculosis* mutants maintain the acid-fastness of the cell wall, these mutants became sensitive to a wider variety of β-lactams than did *M. smegmatis* mutants. Slow penetration of antibiotics through the cell wall has been suggested as a contributor to the intrinsic drug resistance of *M. tuberculosis* (30). Therefore, in *M. tuberculosis*, LM and LAM might play more important roles in restricting the physical pores that allow penetration of β-lactams. Alternatively, the longer doubling time of *M. tuberculosis* may allow higher accumulation levels of β-lactams, making wider varieties of β-lactams effective against the slow-growing pathogen. Other contributing factors, such as β-lactamase and efflux pumps, may also explain the species difference. In particular, the intrinsic resistance of *M. tuberculosis* to β-lactams is well established (31), and *blaC*, the gene encoding β-lactamase, is known to play a dominant role (32). It is possible that β-lactamase and/or efflux pumps have different substrate specificities in *M. smegmatis* and *M. tuberculosis*. Further studies are needed to clarify which of these parameters play dominant roles in the differential antibiotic sensitivities.

We found that both deletion and overexpression of branch-forming α-1,2-mannosyltransferase (MSMEG_4247 or Rv2181) compromised cell wall integrity in *M. smegmatis* and *M. tuberculosis*. While the deletion has a significant impact on cell wall integrity in both species, the effect of overexpression on cell wall integrity was greater, as measured by higher sensitivity to antibiotics. These effects of overexpression are unlikely to be due to the toxic effect of protein overexpression, because overexpression of catalytically inactive enzyme did not affect cell wall integrity in *M. smegmatis* (Fig. 3; Table 1). Furthermore, tetracycline-induced downregulation of *MSMEG_4241* expression, which caused the disappearance of mature LM and LAM, led to similar phenotypes. These data suggest that LM and LAM with shorter mannose backbones have greater impacts on cell wall permeability. In Gram-positive bacteria, polymers known as lipoteichoic acids and wall teichoic acids are thought to play important roles in the maintenance of cell wall integrity (33, 34), and one proposed function is to strengthen the cell wall permeability barrier by filling in the pores and cavities present in the peptidoglycan mesh (35). Our data suggest that LM and LAM may have a similar function and that LM and LAM with shorter mannan backbones are ineffective at fulfilling such functions. A recent study indicated that clinical isolates of *M. tuberculosis* produce a truncated LAM with reduced arabinan and mannan sizes (36). It would be interesting to examine if these phenotypes were produced as a consequence of overexpression of Rv2181 relative to Rv2174 and if these clinical isolates show differences in cell wall permeability.

LAM arabinans from pathogenic species are modified by oligomannose capping, while those from nonpathogenic species are either modified by inositol phosphate or unmodified. Despite a number of studies indicating that oligomannose capping is involved in immune modulation (10, 25), mutant *Mycobacterium marinum* and *Mycobacterium bovis* BCG lacking the mannose cap did not show any defects in infection of zebrafish and mouse models, respectively (37). Therefore, the true functions of the oligomannose cap remain to be determined. In *M. tuberculosis*, Rv2181 is not only involved in the addition of monomannose side chains to the mannan backbone but is also responsible for adding terminal α-1,2-mannoses in the mannose cap structure (15). Therefore, we expect that our *Rv2181* deletion mutant will lack the terminal mannose modifications in addition to the monomannose side chains of the mannan backbone. In the current study, the *Rv2181* deletion mutant infected mice effectively, and its growth in the lung was comparable to that of the wild type. These data are consistent with the previous observations that mannose cap structure does not have a dominant role during host infection.

In contrast to the *Rv2181* deletion mutant, there was a defect in the ability of the Rv2181 overexpression mutant to establish infection. The Rv2181 overexpression mutant showed slightly less effective establishment of infection in the lung and failed to kill mice as effectively as did wild-type *M. tuberculosis*. We noticed that the lung CFU started to decline after 8 weeks in mice infected with the Rv2181 overexpression strain. Although it is beyond the scope of the current study, these data might indicate the role of an acquired immune response. While we cannot exclude the possibility that Rv2181 overexpression affected the mannose cap structure of LAM, this cannot explain the defective cell wall integrity of the equivalent mutant in *M. smegmatis*. Indeed, the MSMEG_4247 overexpression mutant showed increased sensitivity to various antibiotics and macrophage killing, comparable to those of the *M. tuberculosis* mutants. A more likely possibility is that shortening of the mannose backbone has a significant impact on the integrity of the *M. tuberculosis* cell wall and affects the ability of the pathogen to establish infection in mice. Based on our analysis of the MSMEG_4241 Tet-off strain, we predict that inhibition of the orthologous Rv2174 would have similar changes in LM/LAM structures and a similar impact on cell wall integrity in *M. tuberculosis*. We therefore suggest that key enzymes such as Rv2174 in the LM/LAM biosynthetic pathway could be potential targets for TB chemotherapy.

MATERIALS AND METHODS

Mycobacterial strains and culture conditions. *M. smegmatis* mc^{2}155 (38) and derived mutants (14) were grown at 30°C in Middlebrook 7H9 broth (BD, Franklin Lakes, NJ) supplemented with 0.2% (wt/vol) glucose, 0.2% (vol/vol) glycerol, 15 mM NaCl, and 0.05% (vol/vol) Tween 80. Viability was determined by counting CFU on Middlebrook 7H10 agar plates supplemented with 0.2% (wt/vol) glucose, 0.2% (vol/vol) glycerol, and 15 mM NaCl. *M. tuberculosis* H37Rv and derived mutants were grown at 37°C in Middlebrook 7H9 broth supplemented with Middlebrook albumin-dextrose-catalase (ADC) enrichment (BD) and 0.05% (vol/vol) Tween 80 or Middlebrook 7H10 agar supplemented with Middlebrook oleic acid-albumin-dextrose-catalase (OADC) enrichment (BD).

Electron microscopy. Conventional transmission electron microscopy was performed (39). The bacteria were fixed in 2.5% glutaraldehyde and 0.05% ruthenium red in 0.1 M HEPES (pH 7.4) for 2 h on ice and then washed, dehydrated, and embedded in epoxy resin. Ultrathin sections were obtained with an FC6/UC6 ultramicrotome (Leica Microsystems, Tokyo, Japan), counterstained with lead citrate for 10 min, and then observed with a JEM-1011 electron microscope (JEOL, Tokyo, Japan).

Permeability of chemical compounds. The membrane permeability test was performed as described previously (40). Briefly, stationary-phase

TABLE 3 Antibiotic sensitivities of *M. tuberculosis* mutants[a]

Antibiotic class	Antibiotic name	IC_{50} (μg/ml)		
		Wild type	Δ2181+^{Phsp60}2181	Δ2181 + empty vector
Glycopeptide	Vancomycin	4.1 ± 0.6	2.8 ± 0.1	7.8 ± 0.8
Penam	Ampicillin	>800	133 ± 6	247 ± 31
	Carbenicillin	>400	42.8 ± 0.9	62.4 ± 1.8
	Benzylpenicillin	156 ± 4	10.2 ± 0.2	19.0 ± 2.5
Carbapenem	Meropenem	3.3 ± 0.2	1.9 ± 0.1	2.6 ± 0.0
Cephem	Cephalothin	>100	10.7 ± 0.1	17.3 ± 0.6
	Cefamandole	143 ± 11	9.0 ± 0.8	19.2 ± 0.2
	Cefotaxime	15.3 ± 1.6	4.6 ± 0.3	6.8 ± 0.2
	Cefepime	5.4 ± 0.2	3.2 ± 0.1	5.2 ± 0.2
Monobactam	Aztreonam	>200	>200	>200

[a] All data are given as means ± standard deviations from triplicate data except for aztreonam, which was tested in duplicate.

cells were diluted in phosphate-buffered saline (PBS) to an optical density at 600 nm (OD_{600}) of 0.05, and further dilutions were prepared by 10-fold serial dilutions. Three microliters of each diluted solution was spotted onto agar plates containing 0.005% (vol/vol) SDS, 1.25 μg/ml malachite green, or 2.5 μg/ml crystal violet. For tetracycline-inducible strains, 40 ng/ml atc was also added as a supplement. Cells were incubated for 3 days at 37°C.

Acid-fast staining. Cells were stained using the Ziehl-Neelsen method (41). Briefly, cells at logarithmic growth phase were washed twice in PBS, air dried on a slide glass, and fixed by flaming. The slide was then treated sequentially with carbol-fuchsin solution, 3% HCl in ethanol, and 0.3% methylene blue.

Sensitivity to antimicrobials. For the alamarBlue growth assay (Invitrogen, Carlsbad, CA), antimicrobials were serially diluted with Middlebrook 7H9 broth in 96-well microtiter plates, and either *M. smegmatis* or *M. tuberculosis* cells were inoculated at 5×10^4 CFU or 2×10^5 CFU per well, respectively. *M. smegmatis* cells were grown at 30°C for 24 h, mixed with alamarBlue solution, and then incubated for a further 8 h for colorization. The absorbance was then measured at 570 nm. *M. tuberculosis* cells were grown at 37°C for 5 days and incubated with alamarBlue solution for 24 h. Cells were killed by the addition of 25 μl of formalin prior to absorbance measurement.

SDS-PAGE and Western blotting. Cell lysates were prepared by bead beating as described previously (12). Proteins were fractionated by SDS-polyacrylamide gel electrophoresis (SDS-PAGE) (10 to 20% gradient gel) under reducing conditions and blotted onto a polyvinylidene difluoride membrane (Merck Millipore, Tokyo, Japan). The membrane was blocked with 5% skim milk and then incubated with a primary antibody (rabbit antibody against MSMEG_4241, MSMEG_4247, or Rv2181; 1 μg/ml) (14) for 1 h and a secondary antibody (anti-rabbit IgG antibody, horseradish peroxidase conjugated; 1:2,000 dilution; GE Healthcare) for 1 h. The bound probe was visualized by chemiluminescence (PerkinElmer Life Sciences, Yokohama, Japan), and images were captured using a luminescent image analyzer (LAS-4000; Fujifilm, Tokyo, Japan). To detect *M. tuberculosis* Rv2181 by Western blotting, rabbit anti-Rv2181 antibody was raised using a peptide cocktail of MSAWRAPEVGSRLGRRC and CTPQRSLTRGLTPAPTAS and affinity purified.

Lipid extraction and analysis. Lipid extraction was performed as described previously (42). Briefly, lipids were extracted sequentially in chloroform-methanol (2:1, vol/vol) twice and chloroform-methanol-water (1:2:0.8, vol/vol/vol) once. The combined extracts were dried, and lipids were further purified with 1-butanol–water (2:1, vol/vol). For LM/LAM extraction, delipidated pellets were resuspended in Tris-EDTA (pH 6.6)-saturated phenol-water (1:1) and extracted for 2 h at 55°C, and the extract was then further purified by proteinase K digestion followed by octyl-Sepharose column chromatography (GE Healthcare, Tokyo, Japan). LM and LAM were separated by SDS-polyacrylamide gel electrophoresis (10 to 20% gradient gel) and visualized using the ProQ Emerald 488 carbohydrate staining kit (Molecular Probes).

Release and analysis of mycolic acids. Following lipid extraction, cell pellets were resuspended in 10% KOH in 80% aqueous methanol and incubated at 100°C for 5 h. Released mycolic acids were extracted by hexane and converted to methyl esters by refluxing in benzene-methanol-H_2SO_4 (10:20:1, vol/vol/vol) for 2 h. Mycolic acid methyl esters were purified by chloroform-methanol-water (8:4:3, vol/vol/vol) partitioning and separated on a high-performance thin-layer chromatography (HPTLC) plate with a solvent system of hexane-diethyl ether (4:1, vol/vol). Mycolic acid methyl esters were visualized by spraying chromic acid staining solution and baking at 150°C.

THP-1 monocyte cell infection. Infection of THP-1 cells, a human monocyte cell line, was performed according to published protocols (43) with modifications. Briefly, THP-1 cells were grown in RPMI 1640 supplemented with 10% heat-inactivated fetal bovine serum (Thermo), 0.5% RPMI 1640 amino acid solution (Sigma), 0.5% minimal essential medium nonessential amino acids (Invitrogen), 1% 1 mM HEPES (Sigma), 0.1% β-mercaptoethanol (Invitrogen), and 20 μg/ml amikacin (Sigma). THP-1 cells were inoculated in 96-well plates (100-μl volumes) at 1×10^5 cells per well and differentiated in the presence of 50 nM phorbol myristic acid for 1 day. Cells were washed in PBS and resuspended in RPMI 1640 supplemented as described above except for the addition of 10% non-heat-inactivated human serum instead of heat-inactivated fetal bovine serum and omission of amikacin. *M. smegmatis* cells were added at a multiplicity of infection of 1 and incubated at 37°C for 3 h. Extracellular bacteria were removed by washing with PBS. THP-1 cells were incubated further, and at each time point, surviving *M. smegmatis* bacteria were recovered by lysing THP-1 cells in 0.05% SDS and plated for colony counting.

Establishment of tetracycline-inducible strain. To create a Tet-off MSMEG_4241 mutant, pSE100 carrying a revTetR-controlled promoter was used (44). A 5′ fragment of the *MSMEG_4241* gene was amplified from *M. smegmatis* genomic DNA by PCR using the following primer pairs (in which the SphI and NotI restriction enzyme sites, respectively, are underlined): 5′ TTGGAAGCATGCAATGTCCACCCGCAG GC 3′ and 5′ ATTAAGGAATGCGGCCGCTAAGGCACCGAGAGCA GCAG 3′. The PCR fragments were cloned into the SphI and NotI sites of the Tet-off vector. The construct was integrated into the *M. smegmatis* genome by homologous recombination, and a revTet repressor expression vector, pTEK-4S0X (44), was transfected to establish a tetracycline-inducible strain. Control strains carried episomal pTEK-

4S0X only. For induction, growth medium was supplemented with 40 ng/ml atc.

Southern blot analysis. Genomic DNA was extracted as described previously (45). A 10-μg aliquot of digested DNA was resolved by electrophoresis on an 0.8% agarose gel in 1× Tris-acetate-EDTA (TAE) buffer and blotted onto a Hybond N^+ nylon membrane (Amersham Biosciences). Probe hybridization and signal detection were performed as previously described (12). The probe was prepared by PCR amplification of a DNA fragment from *M. smegmatis* genomic DNA using the primer pair 5′ CATACATCGGTCCGGTGTAC 3′ and 5′ AAGGTGTTGACGTT GAGCG 3′ (Fig. 4A).

MALDI-TOF-MS analysis. For MALDI-TOF-MS analysis, 1.0 μg of purified LM/LAM sample was mixed with 1.0 μl of the matrix solution, which consisted of 10 mg/ml 2,5-dihydroxybenzoic acid and 0.1% trifluoroacetic acid in water-acetonitrile (1:1, vol/vol). Samples were analyzed on a Bruker Ultraflex MALDI-TOF/TOF instrument (Bruker Daltonics, Billerica, MA) using reflector mode and in negative mode detection.

Mouse infection. Animal experimentation was carried out in accordance with the guidelines for animal care approved by the National Institute of Infectious Diseases, Japan. C57BL/6 mice (female, 6 weeks old; SLC, Shizuoka, Japan) were maintained under specific-pathogen-free conditions in a biosafety level 3 facility. Mice (12 per group) were infected via intratracheal injection of 5.0×10^4 CFU of *M. tuberculosis* H37Rv suspended in 50 μl PBS. Survival curves were analyzed statistically using a log rank test. At the indicated number of weeks postinfection, lung homogenates were diluted 10^3- to 10^6-fold in PBS and spread on 1% Ogawa-egg medium (Kyokuto Pharmaceutical Industrial, Tokyo, Japan) for colony counting (CFU ± standard deviation, $n = 3$). The CFU values were analyzed statistically using the Mann-Whitney *U* test.

Analysis of infected mouse lungs. Lung tissues from infected mice were fixed in 10% formalin-PBS for histological analysis. The paraffin-embedded sections were stained with hematoxylin and eosin. The cytokine levels in lung homogenates were determined by FlowCytomix (eBioscience, San Diego, CA) using a FACSCalibur flow cytometer (BD, Franklin Lakes, NJ), according to the manufacturer's instructions.

ACKNOWLEDGMENTS

We thank Keiko Kinoshita and Kana Miyanagi for technical assistance. THP-1 cells were kindly provided by Norimitsu Inoue, Osaka Medical Centre for Cancer, Osaka, Japan. Vectors for the Tet-off system (pTEK-4S0X and pSE100) were kindly provided by Dirk Schnappinger, Weill Cornell Medical College, New York, NY.

T.F. was supported by KAKENHI20890114 from the Japan Society for the Promotion of Science (JSPS). Y.S.M. was supported by a Career Development Award from the Human Frontier Science Program and KAKENHI20590441/23590507 from JSPS. T.M., M.A., S.M., and K.K. were supported by Research on Emerging and Re-emerging Infectious Diseases (H23-Sinko-Ippan-008) from the Ministry of Health, Labor and Welfare of Japan.

REFERENCES

1. **World Health Organization.** 2011. Global tuberculosis control: WHO report 2011. World Health Organization, Geneva, Switzerland.
2. **Brennan PJ.** 2003. Structure, function, and biogenesis of the cell wall of *Mycobacterium tuberculosis*. Tuberculosis (Edinb.) **83**:91–97.
3. **Pitarque S, Larrouy-Maumus G, Payré B, Jackson M, Puzo G, Nigou J.** 2008. The immunomodulatory lipoglycans, lipoarabinomannan and lipomannan, are exposed at the mycobacterial cell surface. Tuberculosis (Edinb.) **88**:560–565.
4. **Gilleron M, Quesniaux VF, Puzo G.** 2003. Acylation state of the phosphatidylinositol hexamannosides from *Mycobacterium bovis* bacillus Calmette Guerin and *Mycobacterium tuberculosis* H37Rv and its implication in Toll-like receptor response. J. Biol. Chem. **278**:29880–29889.
5. **Morita YS, Fukuda T, Sena CB, Yamaryo-Botte Y, McConville MJ, Kinoshita T.** 2011. Inositol lipid metabolism in mycobacteria: biosynthesis and regulatory mechanisms. Biochim. Biophys. Acta **1810**:630–641.
6. **Chatterjee D, Hunter SW, McNeil M, Brennan PJ.** 1992. Lipoarabinomannan. Multiglycosylated form of the mycobacterial mannosylphosphatidylinositols. J. Biol. Chem. **267**:6228–6233.
7. **Kaur D, McNeil MR, Khoo KH, Chatterjee D, Crick DC, Jackson M, Brennan PJ.** 2007. New insights into the biosynthesis of mycobacterial lipomannan arising from deletion of a conserved gene. J. Biol. Chem. **282**:27133–27140.
8. **Guerin ME, Korduláková J, Alzari PM, Brennan PJ, Jackson M.** 2010. Molecular basis of phosphatidyl-*myo*-inositol mannoside biosynthesis and regulation in mycobacteria. J. Biol. Chem. **285**:33577–33583.
9. **Kaur D, Guerin ME, Skovierová H, Brennan PJ, Jackson M.** 2009. Biogenesis of the cell wall and other glycoconjugates of *Mycobacterium tuberculosis*. Adv. Appl. Microbiol. **69**:23–78.
10. **Mishra AK, Driessen NN, Appelmelk BJ, Besra GS.** 2011. Lipoarabinomannan and related glycoconjugates: structure, biogenesis and role in *Mycobacterium tuberculosis* physiology and host-pathogen interaction. FEMS Microbiol. Rev. **35**:1126–1157.
11. **Kovacevic S, Anderson D, Morita YS, Patterson J, Haites R, McMillan BN, Coppel R, McConville MJ, Billman-Jacobe H.** 2006. Identification of a novel protein with a role in lipoarabinomannan biosynthesis in mycobacteria. J. Biol. Chem. **281**:9011–9017.
12. **Morita YS, Sena CB, Waller RF, Kurokawa K, Sernee MF, Nakatani F, Haites RE, Billman-Jacobe H, McConville MJ, Maeda Y, Kinoshita T.** 2006. PimE is a polyprenol-phosphate-mannose-dependent mannosyltransferase that transfers the fifth mannose of phosphatidylinositol mannoside in mycobacteria. J. Biol. Chem. **281**:25143–25155.
13. **Kaur D, Berg S, Dinadayala P, Gicquel B, Chatterjee D, McNeil MR, Vissa VD, Crick DC, Jackson M, Brennan PJ.** 2006. Biosynthesis of mycobacterial lipoarabinomannan: role of a branching mannosyltransferase. Proc. Natl. Acad. Sci. U. S. A. **103**:13664–13669.
14. **Sena CB, Fukuda T, Miyanagi K, Matsumoto S, Kobayashi K, Murakami Y, Maeda Y, Kinoshita T, Morita YS.** 2010. Controlled expression of branch-forming mannosyltransferase is critical for mycobacterial lipoarabinomannan biosynthesis. J. Biol. Chem. **285**:13326–13336.
15. **Kaur D, Obregón-Henao A, Pham H, Chatterjee D, Brennan PJ, Jackson M.** 2008. Lipoarabinomannan of *Mycobacterium*: mannose capping by a multifunctional terminal mannosyltransferase. Proc. Natl. Acad. Sci. U. S. A. **105**:17973–17977.
16. **Mishra AK, Alderwick LJ, Rittmann D, Tatituri RV, Nigou J, Gilleron M, Eggeling L, Besra GS.** 2007. Identification of an alpha(1→6) mannopyranosyltransferase (MptA), involved in *Corynebacterium glutamicum* lipomannan biosynthesis, and identification of its ortholog in *Mycobacterium tuberculosis*. Mol. Microbiol. **65**:1503–1517.
17. **Chatterjee D, Khoo KH, McNeil MR, Dell A, Morris HR, Brennan PJ.** 1993. Structural definition of the non-reducing termini of mannose-capped LAM from *Mycobacterium tuberculosis* through selective enzymatic degradation and fast atom bombardment-mass spectrometry. Glycobiology **3**:497–506.
18. **Chatterjee D, Lowell K, Rivoire B, McNeil MR, Brennan PJ.** 1992. Lipoarabinomannan of *Mycobacterium tuberculosis*. Capping with mannosyl residues in some strains. J. Biol. Chem. **267**:6234–6239.
19. **Venisse A, Berjeaud JM, Chaurand P, Gilleron M, Puzo G.** 1993. Structural features of lipoarabinomannan from *Mycobacterium bovis* BCG. Determination of molecular mass by laser desorption mass spectrometry. J. Biol. Chem. **268**:12401–12411.
20. **Dinadayala P, Kaur D, Berg S, Amin AG, Vissa VD, Chatterjee D, Brennan PJ, Crick DC.** 2006. Genetic basis for the synthesis of the immunomodulatory mannose caps of lipoarabinomannan in *Mycobacterium tuberculosis*. J. Biol. Chem. **281**:20027–20035.
21. **Sassetti CM, Boyd DH, Rubin EJ.** 2003. Genes required for mycobacterial growth defined by high density mutagenesis. Mol. Microbiol. **48**: 77–84.
22. **Briken V, Porcelli SA, Besra GS, Kremer L.** 2004. Mycobacterial lipoarabinomannan and related lipoglycans: from biogenesis to modulation of the immune response. Mol. Microbiol. **53**:391–403.
23. **Gilleron M, Jackson M, Nigou J, Puzo G.** 2008. Structure, biosynthesis, and activities of the phosphatidyl-*myo*-inositol-based lipoglycans, p 75–105. *In* Daffe M, Reyrat JM (ed), The mycobacterial cell envelope. ASM Press, Washington, DC.
24. **Schlesinger LS, Azad AK, Torrelles JB, Roberts E, Vergne I, Deretic V.** 2008. Determinants of phagocytosis, phagosome biogenesis and autophagy for *Mycobacterium tuberculosis*, p 1–22. *In* Kaufmann SHE, Britton WJ (ed), Handbook of tuberculosis: immunology and cell biology. Wiley-VCH Verlag, Weinheim, Germany.

25. **Torrelles JB, Schlesinger LS.** 2010. Diversity in *Mycobacterium tuberculosis* mannosylated cell wall determinants impacts adaptation to the host. Tuberculosis (Edinb.) **90**:84–93.
26. **Goude R, Amin AG, Chatterjee D, Parish T.** 2008. The critical role of *embC* in *Mycobacterium tuberculosis*. J. Bacteriol. **190**:4335–4341.
27. **Torrelles JB, DesJardin LE, MacNeil J, Kaufman TM, Kutzbach B, Knaup R, McCarthy TR, Gurcha SS, Besra GS, Clegg S, Schlesinger LS.** 2009. Inactivation of *Mycobacterium tuberculosis* mannosyltransferase *pimB* reduces the cell wall lipoarabinomannan and lipomannan content and increases the rate of bacterial-induced human macrophage cell death. Glycobiology **19**:743–755.
28. **Podobnik M, Tyagi R, Matange N, Dermol U, Gupta AK, Mattoo R, Seshadri K, Visweswariah SS.** 2009. A mycobacterial cyclic AMP phosphodiesterase that moonlights as a modifier of cell wall permeability. J. Biol. Chem. **284**:32846–32857.
29. **Fontán P, Aris V, Ghanny S, Soteropoulos P, Smith I.** 2008. Global transcriptional profile of *Mycobacterium tuberculosis* during THP-1 human macrophage infection. Infect. Immun. **76**:717–725.
30. **Chambers HF, Moreau D, Yajko D, Miick C, Wagner C, Hackbarth C, Kocagöz S, Rosenberg E, Hadley WK, Nikaido H.** 1995. Can penicillins and other beta-lactam antibiotics be used to treat tuberculosis? Antimicrob. Agents Chemother. **39**:2620–2624.
31. **Iland CN.** 1946. The effect of penicillin on the tubercle bacillus. J. Pathol. Bacteriol. **58**:495–500.
32. **Flores AR, Parsons LM, Pavelka MS, Jr..** 2005. Genetic analysis of the beta-lactamases of *Mycobacterium tuberculosis* and *Mycobacterium smegmatis* and susceptibility to beta-lactam antibiotics. Microbiology **151**: 521–532.
33. **Peschel A, Vuong C, Otto M, Götz F.** 2000. The D-alanine residues of *Staphylococcus aureus* teichoic acids alter the susceptibility to vancomycin and the activity of autolytic enzymes. Antimicrob. Agents Chemother. **44**:2845–2847.
34. **Sieradzki K, Tomasz A.** 2003. Alterations of cell wall structure and metabolism accompany reduced susceptibility to vancomycin in an isogenic series of clinical isolates of *Staphylococcus aureus*. J. Bacteriol. **185**: 7103–7110.
35. **Weidenmaier C, Peschel A.** 2008. Teichoic acids and related cell-wall glycopolymers in Gram-positive physiology and host interactions. Nat. Rev. Microbiol. **6**:276–287.
36. **Torrelles JB, Knaup R, Kolareth A, Slepushkina T, Kaufman TM, Kang P, Hill PJ, Brennan PJ, Chatterjee D, Belisle JT, Musser JM, Schlesinger LS.** 2008. Identification of *Mycobacterium tuberculosis* clinical isolates with altered phagocytosis by human macrophages due to a truncated lipoarabinomannan. J. Biol. Chem. **283**:31417–31428.
37. **Appelmelk BJ, den Dunnen J, Driessen NN, Ummels R, Pak M, Nigou J, Larrouy-Maumus G, Gurcha SS, Movahedzadeh F, Geurtsen J, Brown EJ, Eysink Smeets MM, Besra GS, Willemsen PT, Lowary TL, van Kooyk Y, Maaskant JJ, Stoker NG, van der Ley P, Puzo G, Vandenbroucke-Grauls CM, Wieland CW, van der Poll T, Geijtenbeek TB, van der Sar AM, Bitter W.** 2008. The mannose cap of mycobacterial lipoarabinomannan does not dominate the *Mycobacterium*-host interaction. Cell. Microbiol. **10**:930–944.
38. **Snapper SB, Lugosi L, Jekkel A, Melton RE, Kieser T, Bloom BR, Jacobs WR, Jr.** 1988. Lysogeny and transformation in mycobacteria: stable expression of foreign genes. Proc. Natl. Acad. Sci. U. S. A. **85**:6987–6991.
39. **Bleck CK, Merz A, Gutierrez MG, Walther P, Dubochet J, Zuber B, Griffiths G.** 2010. Comparison of different methods for thin section EM analysis of *Mycobacterium smegmatis*. J. Microsc. **237**:23–38.
40. **Banaei N, Kincaid EZ, Lin SY, Desmond E, Jacobs WR, Jr, Ernst JD.** 2009. Lipoprotein processing is essential for resistance of *Mycobacterium tuberculosis* to malachite green. Antimicrob. Agents Chemother. **53**: 3799–3802.
41. **Shoub HL.** 1923. A comparison of the Ziehl-Neelsen and Schulte-Tigges methods of staining tubercle bacilli. J. Bacteriol. **8**:121–126.
42. **Morita YS, Patterson JH, Billman-Jacobe H, McConville MJ.** 2004. Biosynthesis of mycobacterial phosphatidylinositol mannosides. Biochem. J. **378**:589–597.
43. **Hinchey J, Jeon BY, Alley H, Chen B, Goldberg M, Derrick S, Morris S, Jacobs WR, Jr, Porcelli SA, Lee S.** 2011. Lysine auxotrophy combined with deletion of the SecA2 gene results in a safe and highly immunogenic candidate live attenuated vaccine for tuberculosis. PLoS One **6**:e15857. http://dx.doi.org/10.1371/journal.pone.0015857.
44. **Guo XV, Monteleone M, Klotzsche M, Kamionka A, Hillen W, Braunstein M, Ehrt S, Schnappinger D.** 2007. Silencing *Mycobacterium smegmatis* by using tetracycline repressors. J. Bacteriol. **189**:4614–4623.
45. **Jeevarajah D, Patterson JH, Taig E, Sargeant T, McConville MJ, Billman-Jacobe H.** 2004. Methylation of GPLs in *Mycobacterium smegmatis* and *Mycobacterium avium*. J. Bacteriol. **186**:6792–6799.

学術

綜説

結核とその制圧を目指した研究

新潟大学大学院医歯学総合研究科細菌学分野
松　本　壮　吉

はじめに

はじめまして、平成25年９月１日付けで新潟大学医学部医学科細菌学教室・新潟大学大学院医歯学総合研究科細菌学分野の教授を拝命いたしました松本壮吉と申します。新潟県医師会の皆様にこの場をかりてご挨拶申し上げます。私は1968年、長崎県対馬で生まれ、1992年に長崎大学歯学部を卒業、同大学院で結核・抗酸菌症を学ぶ機会をいただき、1999年から米国国立衛生研究所（NIH）結核部門にて博士研究員、2002年から大阪市立大学大学院医学研究科細菌学分野にて講師・准教授として結核・抗酸菌症の研究に携わって参りました。細菌学はロベルト・コッホの時代からの歴史のある学問である一方、現在も薬剤耐性や院内感染問題など臨床と直結する領域です。新潟に研究室を開かせていただき微力ながら皆様のお役にたつようなことができればと思います。本稿では、専門にしております結核について、歴史と現状、病態形成のしくみ、現在の研究動向と目指す成果についてご紹介申し上げご挨拶に代えさせていただきます。

結核（症）の歴史的な変遷

現在、結核の痕跡として最も古いものは、イスラエル沖の地中海で2008年発見された9,000年前の２体の人骨に残る脊椎カリエスですが[1]、人型結核菌（*Mycobacterium tuberculosis*）の誕生は更にさかのぼり、ゲノム解析によると約５－10万年前のアフリカにおける人類の誕生と同時期に近縁菌より進化して病原性を獲得し、人の出アフリカに伴って世界中に伝播したと推測されています[2]。

アフリカ東岸には、現在も古代結核菌の末裔と目される結核菌 *Mycobacterium canetti* が認められ、しばしば人に結核をおこしています。国内で分離される結核菌がラフ型集落を形成するのに対し、*M. canetti* はスムース型の一般細菌のような集落を形成するのが特徴です。集落の形状からすると、より病原性を獲得し人に寄生することに成功した人型結核菌は、その時にスムース型集落の形成に必要ななんらかの細胞壁成分を喪失した可能性があります。それが強い病原性の獲得とも関係があるかもしれませんが、その謎はまだ解かれていません。

戦後の急速な結核罹患率の低下から惰性的に制圧されると楽観された時期もありましたが、AIDS の蔓延によって発展途上国における結核の脅威は増大し、さらに先進国においても多剤耐性結核菌の出現などが災いして日本を含め罹患率が再上昇する国もあらわれました。WHO 等の尽力で結核の罹患率は低下傾向にありますがそれでも、2011年に870万人が結核を発症し、140万人が死亡しています。国内では、平成23年に22,681人が結核を発症し、2,166人が死亡しました。このように結核は、代表的な再興感染症で、現在も世界／国内ともに最大級の細菌感染症です。

結核病態の形成と脂質成分

結核（tuberculosis）という病名は肉芽腫による小結節（tubercule）に由来しています。小結節の実態は、肉芽種で、結核病変は結核菌感染に特徴的な特異性炎です。これは、宿主が完全に菌を殺傷することができないこと、また菌体成分の消化／吸収に時間を要することが原因です。中心部に菌を貪食したマクロファージが集積しその周囲を支援するＴ細胞が取り囲む、あたかも強固な城を攻略しているような病理組織像が肉芽腫です。戦いは長期戦に入り、中心はやがて壊死し、陥落して空洞化していきます。

この特徴的病変は菌の毒素によるとの考えが主流であった時に刀根山病院の山村雄一（後に大阪大学）は、菌体成分に対する宿主応答が結核特異性炎の実体であることを動物モデルを使って示しました[3]。この研究成果は、宿主応答を調節する生体分子、すなわち種々のサイトカインの発見に繋がり、後の日本における免疫学の隆盛を促します。巨大な肉芽腫は肺の組織破壊を招き個体の死を招来しますが、肉芽腫形成は基本、宿主の防御応答で、好気性である結核菌の増殖を主に酸素を遮断することで停止させる"苦肉の策"といえます。

結核菌を液体培地で培養すると紐状の形態をとりながら増殖します。馬の尻尾に形状が似ることから、これをコード形成とよび、これに関わるであろうと同定された糖脂質の一つがコードファクターと呼ばれていました。コードファクターの構造が解かれると、２つのミコール酸がトレハロースに縮合したトレハロースダイマイコレート（TDM）であることが分かりました。ミコール酸は、抗酸性と関わる抗酸菌に特有の長鎖脂肪酸で、TDMは、結核菌の細胞壁表層を覆う主要な糖脂質でした。

山村等は細胞壁画分に強い免疫賦活能を見いだしましたが、私の恩師であります小林等も示したように、その中にはコードファクターが含まれていました[4),5)]。現在では、コードファクターによるコード形成能は否定的ですが、単独で肉芽腫を形成する強い免疫原性が知られ研究されてきました。九州大学の山崎　晶等は、自己抗原を認識するCタイプレクチンを研究していたところ、その一つのMincleが、コードファクターを認識することを発見しました[6)]。日本人研究者によってコードファクターの発見から約50年かけてようやくそのレセプターが同定されたことになります。

結核菌はグラム陽性菌ですが、驚いたことに最近、グラム陰性菌のように外膜が存在することが分かってきました。外膜はTDMなどミコール酸を含んだ糖脂質やリポアラビノマンナン（LAM）などから形成されているようです。結核菌の細胞重量の約30％は細胞壁で、この重厚な脂質が抗酸性をあらわし、また生体内において宿主の攻撃から菌を保護します。

結核菌はミコール酸以外にも複数の特徴的な糖脂質を産生し宿主応答をかく乱するようです。例えばLAMは別のCタイプレクチンであるdendritic cell-specific ICAM-3 grabbing non-integrin（DC-SIGN）というレセプター刺激を介して、Toll-like receptor（TLR）刺激による樹状細胞の活性化を抑制することが知られています。DC-SIGNは、HIVも利用するレセプターで、HIVに対する免疫不応答を誘導します。結核菌やHIVなど代表的な感染病原体がともに同じCタイプレクチンを免疫抑制に利用していることになります。

蛋白性の病原因子

結核菌は重厚な細胞壁をまとって宿主細胞の攻撃に備えていますが、それでもTLRとビタミンD_3刺激によって誘導される抗菌ペプチド、オートファジー、NADPHオキダーゼ依存的に産生されるヒドロキシラジカル、NO合成酵素によって作られる一酸化窒素など、宿主は複数の武器によって結核菌を殺傷することができます。菌はそれに対抗して複数の蛋白性病原因子を産生し細胞内生存を可能にしているようです。

結核菌の最も主要な生存戦略として認知されていたのが、結核菌を貪食した食胞、すなわちファゴゾーム（P）と、殺菌効果のあるリソソーム（L）の融合を阻止する、いわゆるP-L fusionの阻害です。結核菌はアンモニアを産生したり、プロトン輸送蛋白質によってファゴゾーム内のpH低下を阻止し、さらに分泌型のリン酸化酵素によって細胞内の膜輸送系に作用してP-L fusionを抑制すると言われています。

一方最近の報告から、ヒトのマクロファージや樹状細胞では感染後速やかなP-L fusionが生じるが、結核菌は蛋白質the 6 kDa early secretory antigenic target of *M. tuberculosis*（ESAT6）を産生してファゴライソソーム膜孔を障害し細胞質に逃れることも報告されるようになりました[7)]。ESAT6はthe 10 kDa culture filtrate protein（CFP10）蛋白質との２量体で結核菌から分泌されます。結核ワクチンBCGにはこのESAT6とCFP10が欠落しており、BCGの弱毒化を一部説明しています。また臨床的には、ESAT6とCFP10に対する免疫応答の有無で結核菌感染者を

特異的に検知できるキットに利用されており（商品名：クゥオンティフェロン、QFT など）BCG 接種で陽転化するツベルクリン試験に代わりつつあります。

このクゥオンティフェロン試験に利用されている蛋白質 ESAT6と CFP10が、結核菌の殺傷機構のひとつであるオートファージーの誘導にも関わっているようです。もともとオートファージーは、細胞質の老廃物などを飢餓などをきっかけに分解する自食のシステムですから、ESAT6と CFP10を利用して細胞質に逃れた結核菌をとらえて消化する働きがあるようです。ただ、ESAT6と CFP10を欠失させた結核菌は病原性が低下しますから、ESAT6と CFP10によってオートファージーが誘導されても、結核菌はそれ以上に、細胞内で増殖する術を持っているようです。

結核菌の生活環と潜在性結核

述べてきましたように、結核菌は細胞壁を基本バリアとして病原因子を分泌し宿主の殺菌機構に抵抗します。通常、結核菌と現人類（宿主）の戦いは宿主優勢で発病せず“よい勝負”ですが、宿主が感染した菌を駆逐することもありません。その結果、結核菌は感染しているが無症候である人が多く、人類の1/3に達しているといわれています。日本人の場合、５人に１人が感染者であるといいます。この無症候感染者で、抵抗性の減衰、HIV 感染、糖尿病など抵抗力の低下が生じると、菌が増殖を開始し結核を発症することになります。これを内因性再燃による二次結核と呼びます。内因性再燃は、あたかも寄生宿主の命が尽きると判断した結核菌が、再増殖して病気をおこし、咳と共に感染宿主を離れ、新たな住み処に移っていく様ととらえることができます（図１）。

このように無症候感染者は、将来結核を発症する可能性があることから、活動性結核に対して潜在性結核と呼ばれ、注視されるようになりました。前述のように、結核菌の住み処は人で、その他の動物や一般環境中では一般に生存しません。したがって活動性結核に加え、病原体の源泉である潜在性結核に対処することが結核の根本的な対策につながると私は考えています。

ワクチン開発の試み

予防や治療の介入によって結核を制圧するために、新規のワクチンや薬剤の開発が鍵と考えられます。現行ワクチン BCG は小児の粟粒結核をおよそ60-80％予防する効果があります。一方、インドにおける10万人規模の調査で、BCG 接種者の追跡試験を行った結果、“効果無し”と判定が下されたように[8]、成人の肺結核に対する効果は低調です。そのため日本でも平成15年を境に小中学校における BCG の再接種は廃止されてしまいました。

世界的に結核ワクチンの開発が進んでいますが、分類すると　①防御抗原や免疫賦活物質のみを投与する成分ワクチンや DNA ワクチン　②BCG を改良する組み換え BCG　③結核菌自体を弱毒化するオークソトロフに分けることができます。前述のように結核菌は生体内の生存能にたけており、また防御免疫を獲得したはずの既感染者への再感染もあることからワクチン開発はかなりの困難が予測されます。

結核ワクチン開発に関して、やはり多くの研究者が最初に行ったことは、BCG を凌駕するよう

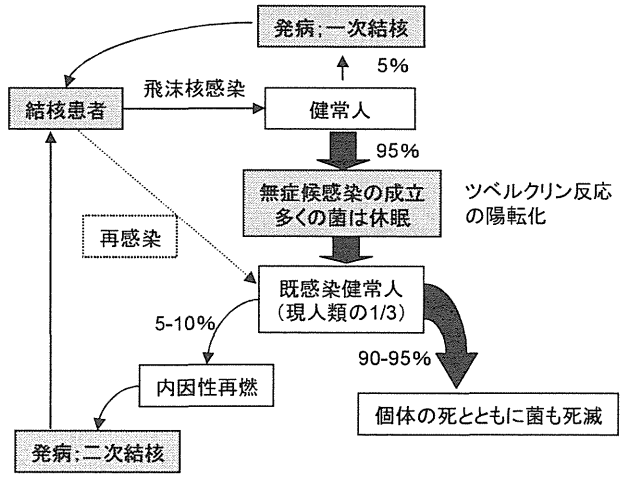

図１　結核菌の生活環との結核の発症

結核患者由来の飛沫が空中にて乾燥し菌を含んだ飛沫核となり、健常人もしくは既感染者（再感染）の肺胞に到達して感染が成立する。この時、感染者の約５％が一次結核を発症する。残る95％は発病しないが、菌は生体から排除されずに無症候感染が成立する。無症候感染者は現人類の1/3にのぼり、その５-10％が終生の間に結核を発病する（二次結核）。また、HIV の感染は二次結核の発症率を約10倍まで上昇させる。